Planetary Circulations: 1. Barotropic Representation of Jovian and Terrestrial Turbulence

GARETH P. WILLIAMS

Geophysical Fluid Dynamics Laboratory/NOAA, Princeton University, Princeton, NJ 08540

(Manuscript received 2 December 1975, in final form 13 April 1978)

ABSTRACT

We seek the formative processes of the planetary circulations of Jupiter and Saturn. The study concentrates on examining whether processes known to control the terrestrial circulation, namely, two-dimensional turbulence and baroclinic instability, can produce Jovian circulations under Jovian conditions. The first numerical model involves a spherical barotropic vorticity equation subjected to a stochastic representation of baroclinic processes. The resulting solutions suggest that a strong affinity exists between the Jovian and terrestrial circulations. This leads to a reevaluation of terrestrial circulation theory from the broader perspective of parameter space.

The solutions in the Jovian regime support the hypothesis that a variation of the Rhines effect—an interaction of the two-dimensional turbulence cascade and Rossby wave propagation—creates the pseudo-axisymmetry and scale $L_\beta=\pi(2U/\beta)^{\frac{1}{2}}$ of the bands (U is the rms zonal velocity, and β the northward gradient of the Coriolis force). The anisotropy of the interaction produces zonally oriented flows, composed of a series of alternating easterly and westerly jets, between which lie characteristic ovals. Equatorial jets occur readily when vorticity sources that lie symmetrically about the equator act on the atmosphere. Frictionally induced Ekman circulations provide a possible mechanism for cloud formation.

Integrations with terrestrial parameters support Kuo's (1951) forced vorticity-transfer theory for the Earth's circulation: westerly jets form in the forced midlatitude zones, and Rossby-wave propagation from those zones causes the broad easterly trade winds. Enstrophy cascade and β effects control the formation of momentum converging eddy patterns. L_β also provides a measure of the width of the terrestrial jet. Cascade blocking by a stronger surface drag prevents terrestrial flows from approaching the same degree of zonality as Jovian ones.

Jupiter also appears to be dynamically equivalent to a hypothetical (or primeval) global ocean that has neither continental boundaries nor surface winds.

1. Introduction

This three-part study is concerned with trying to deduce the fundamental causes of the global circulations of the atmospheres of Jupiter and Saturn. The approach adopted is one of evaluating the behavior of known terrestrial processes under Jovian conditions, rather than of seeking new dynamical mechanisms.

The primary hypothesis made is that the major Jovian characteristics—the axisymmetry and scale of the bands, the zonal currents, the waves and eddies—are all essentially a feature of two-dimensional turbulence on a rapidly rotating planet, with the turbulence being energized by baroclinic instability. To reinforce this supposition, and delineate the relation between the terrestrial and Jovian regimes, the original study (Williams, 1975a,b) has been broadened to include an examination of how the Earth's circulation varies in parameter space. In this regard, a major concern has been to isolate the mechanism that determines the scale of the terrestrial jet—to explain why only one jet occurs in each hemisphere—and to understand why the jets are less zonal than their Jovian counterparts.

This study of planetary turbulence begins with an examination, in the Jovian and terrestrial regimes, of atmospheric responses that are quasi-barotropic.[1] We do not believe that either atmosphere is inherently barotropic, only that on certain scales of space and time, the barotropic exchanges determine certain features. A practical advantage of this assumption is that it involves primarily the horizontal components of motion, and as such does not depend crucially on the vertical structure of the atmosphere—details of which remain obscure for Jupiter. Nonbarotropic effects are represented statistically, using a stochastically forced barotropic scheme to imitate the full baroclinic behavior. Such a formulation is not truly barotropic, and the forced barotropic scheme can be said to provide a barotropic *representation*[2] of the more complex baroclinic

[1] The term barotropy is used in the dynamical context to denote quasi-nondivergent horizontal flow.

[2] "Representation is a compromise with chaos" (Bernard Berenson in *Seeing and Knowing*, 1953, Chapman and Hall, London).

system. This reversion to quasi-barotropic models is not regressive, but provides an essential simplification in understanding zonal flow formation.

Although the interaction of two-dimensional turbulence and Rossby-wave propagation control the largest scales, processes imitated by the stochastic forcing determine energy supply and smaller scale activity. The solutions indicate that the most realistic flows occur under the influence of vorticity sources of a scale comparable to the Jovian half-band width; baroclinic instability provides the most probable candidate for such a vorticity source. This leads us to examine, in Part 2, quasi-geostrophic baroclinic turbulence, using the classical circulation model of Phillips (1956) with Jovian parameters. The baroclinic model explains items not covered by the forced barotropic model: temperature distribution, location of energy conversion, baroclinic length scales, frontogenesis, Great Red Spot, polar regime transition, long-term variation and equilibration. In Part 3, evaluation of the same model for parameter variations in the terrestrial regime clarifies the connection between the Jovian and terrestrial regimes, and broadens the perspective on the terrestrial atmospheric circulation.

To illustrate the relevance and necessity of the quasi-barotropic and baroclinic turbulence hypotheses, we review—in a prelude to all three studies—the basic problems and theories of the circulations of Jupiter (Section 2) and the Earth (Section 3). In Section 4, those turbulence concepts that help explain important aspects of the circulations are reviewed from a planetary perspective. In particular, the Rhines effect will be discussed in detail as it provides a basis for much of this work, and a unifying principle whereby many circulations may be discussed within the same theoretical framework. A digression, in Section 5, explores the relation, if any, between the general turbulence concepts and specialized theories for the Great Red Spot.

2. The Jovian problem

For Jupiter, the main items requiring explanation are the regularity with which the cloud bands parallel the equator and the motions within them. Analyses of eddy motion suggest that the circulation consists of a series of alternating easterly and westerly jets, with velocities of approximately 100 m s^{-1} near the equator and of 20 m s^{-1} at higher latitudes (Chapman, 1969). Distinctive shears exist across the bands such that within zones (light colored bands) and belts (dark colored bands) westerly motion is associated with the poleward edges of zones and the equatorward edges of belts, with easterly motion occurring elsewhere (Hess and Panofsky, 1951). This correlation provides a strong dynamical constraint on models of the *vertical* structure of the circulation. The bands fluctuate in width and color substantially from year to year and vanish completely poleward of 50° latitude. Well-defined oval-shaped disturbances and waves, which last from a week to several months, arise within the bands.

Most of the proposed explanations of the Jovian circulation have one idea in common—that an instability process favoring the axisymmetric mode produces the banded form. The current debate over the cause of the Jovian circulation revolves around three such axisymmetric instabilities (convective, radiative and inertial) and the planetary turbulence hypothesis (Williams, 1975b), to be discussed herein. All of the instability mechanisms have serious disadvantages in practical application to Jupiter and Saturn.

The main drawback, in applying the Solberg symmetric baroclinic instability to Jupiter (Stone, 1967, 1971), lies in the vanishingly small length scales favored by the mechanism (McIntyre, 1970a; Walton, 1975)—a feature shared with the convective instability. Furthermore, the instability only occurs in a highly restricted range of Richardson number. Although the process has been reproduced numerically in the laboratory annulus context (Williams, 1968, 1970), doubts exist as to whether a stable realization is possible under planetary conditions (Hoskins, 1974). The character of the disturbances, with downward motion correlated to westward flow, conflicts with observation.

Although the anisotropic-convection model for a uniformly heated planet (Rossby, 1945; Williams and Robinson, 1973) appears to reproduce the observed mean flows and correlations, it does so under unsatisfactory conditions. In particular, the length scales depend on a poorly understood parameterization of convective turbulence, and the maintenance of such convection requires excessive heat. The instability favors the axisymmetric mode only at lower Rayleigh numbers; however, if the parameterizations are regarded as a representation of the large-scale eddies (as in statistical circulation models), then the question of zonal stability lacks meaning.

The radiative instability mechanism (Gierasch, 1973) invokes a coupled radiative-dynamical cause to band formation—implying that dynamics alone cannot suffice. An *ad hoc* water cloud treatment that does not apply to the Earth system and characteristic scales that depend on this parameterization constitute the main disadvantages of this original theory. In practice, the instability has uncompetitive time scales and the existence of water clouds, banded or otherwise, has not been established.

3. Developments in circulation theory

Our perception of the circulations of the Earth's atmosphere and oceans has altered, from the classical view involving mean circulation concepts, to one in which the unsteady turbulent aspects of the flow predominate; a similar transformation of Jovian circulation theory is required. Consideration of comparative atmospheres raises new questions—concerning the parame-

tric behavior of circulations—with which modern theory must deal.

a. Classical theory

The mean meridional-cell theory of circulation formation assumed the prevalence of a conserved exchange of angular momentum in the meridional plane; the modern view considers the exchange of vorticity or potential vorticity in the horizontal plane as the responsible process. The earlier theory was eventually discarded because it was associated with too large a transfer of angular momentum.

With an emphasis on horizontal turbulent exchanges, Rossby's (1947, 1949) (barotropic) vorticity equalization theory attempted to rationalize the poleward transfer of angular momentum. Rossby further suggested that such theory should be relevant to the formation of the Jovian equatorial circulation, an idea that was taken up by Hess (1952). The inadequacies of this theory were explained when the discovery of baroclinic instability (quasi-horizontal convection) (Charney, 1947; Eady, 1949) revealed that the major formative sources of momentum and vorticity are created in the free atmosphere, and not, as previously supposed, at the surface.

In retrospect, the misconceptions in classical theory can be attributed to three mistaken assumptions: 1) that some motion-related quantity, angular momentum or vorticity, governed the flow and the requirement for heat transfer was secondary; 2) that boundary sources of momentum or vorticity, not internal sources, caused the flow; and 3) that vertical exchange processes were greater than or equal to the horizontal processes in importance. This last conflict arises out of the uniquely strong interaction between the atmosphere and the Earth's surface; the oceanic and Jovian systems exhibit a weaker interaction and a more obvious dominance of horizontal processes.

b. Modern theory

In the first "modern" description of the terrestrial circulation, Eady (1950) recognized the fundamental role of turbulence in the circulation, and regarded the derivation of its cause and properties with respect to the predominating horizontal eddy transports of heat and angular momentum as the main problem. The defining of available potential energy (Lorenz, 1955) clarified the energetic properties of the eddies and mean flow components. The numerical study of Phillips (1956) supported the Eady-Lorenz view of the circulation and made it clear that potential vorticity is the primary distributive variable governing the circulation.

The meridional circulations are secondary effects as far as heat transfer is concerned; they act mainly to transfer angular momentum vertically (Eady, 1950), thereby fulfilling the surface drag's main role, that of limiting the amplitude of the disturbances and the zonal currents that result from their activity. The lack of mean meridional circulations, when our numerical models omit surface drag, bears out Eady's view.

The need to characterize a circulation as having either strong (Earth) or weak (ocean, Jupiter) surface interactions is essential to understanding its form.[3] On Earth, the strong surface drag prevents the zonal flow from evolving far from the Hadley state, thus obscuring the atmosphere's inertial response. The tendencies of a free atmosphere are more clearly revealed in the weakly dissipative Jovian regime where the evolved flow bears no resemblance at all to the axisymmetric state, thus revealing the irrelevance of the Hadley stability problem.

c. Representational theory

To avoid the complexity of baroclinic circulation models, Kuo (1950, 1951, 1953) suggested that for certain dynamical problems, the atmosphere can be regarded as being controlled by barotropic vorticity exchanges and that the internal forcing effects of baroclinic processes could be implicitly represented.

Kuo supposed that vorticity concentrations occur (due to the baroclinic divergence term) in a zonal belt, with equal amounts of cyclonic ($\zeta>0$) and anticyclonic vorticity. The vorticity equation, multiplied by $v\cos\theta$ and integrated over a fluid area A, on whose boundaries v vanishes, becomes

$$\int\int_A \zeta\cos\theta\frac{dv}{dt}dA=\int\int_A v^2(f+\zeta)_y\cos^2\theta dA \qquad (1)$$

(see Section 6 for notation). The correlation between vorticity and acceleration indicates a tendency for vorticity transfer in the direction opposite to the gradient of absolute vorticity. Thus, vortices migrate to latitudes with their particular absolute vorticity: cyclones move poleward and anticyclones equatorward.

As a result of such vortex partitioning, an increased vorticity gradient occurs within the region of active disturbances and a decreased gradient beyond. The resulting poleward transfer of vorticity redistributes existing vorticity and implies a change in the mean zonal flow, the equation for which,

$$\bar{u}_t=\overline{v\zeta}, \qquad (2)$$

indicates that westerly winds will grow within the disturbed zone and easterly currents without. By applying Taylor's (1915) vorticity flux theory these easterly currents can be shown to favor a uniform distribution.

[3] The term surface is used in the Jovian context to denote a sublayer with a different mode of existence.

The theory transforms Eq. (2) into the form

$$\bar{u}_t = -\frac{\beta}{2}\frac{D}{Dt}\overline{y_r^2}, \tag{3}$$

where y_r is the meridional displacement from a latitude of zero relative vorticity (Fjortoft, 1950; Arakawa, 1961; Bretherton, 1966; Dickinson, 1969). For small convective contributions, this exact equation approximates to

$$\bar{u} = -\tfrac{1}{2}\beta\overline{y_r^2} \tag{4}$$

(Rhines, 1977), indicating the tendency toward uniformity and the primary role of β in zonal flow generation.

The importance of absolute vorticity transfer in the actual, complex scheme of atmospheric momentum transfer is also substantiated by Green's (1970) statistical circulation model. In this, transfer coefficients $K_{1,2}$ are used, with reasonable justification, for the quasi-conservative heat and potential vorticity quantities to yield the momentum flux equation for the two-layer model

$$(\overline{u'v'})_y = K_1(f+\zeta)_y - \lambda^2\hat{\psi}_y h(\partial K_1/\partial z) - fK_2, \tag{5}$$

where λ^{-1} is the Rossby radius of deformation and $\hat{\psi}\equiv\psi_1-\psi_3$ the streamfunction differential (temperature) over the scale height h. The relationship between the first two terms resembles that implied by Kuo's theory.

By emphasizing horizontal exchanges and by neglecting surface effects completely, Kuo was led to the cause of the basic circulation characteristics—the partitioning of momentum into easterly and westerly components by the forcing effect of vortex separation. However, the growth and decline of the eddies, through their connection with the baroclinic component of mean flow, represent an additional factor whose explanation defines a more complex model of the circulation than that of a statistically driven zonal flow. Nonetheless, for certain phenomena and for remote atmospheres in particular, the simpler definition provides a meaningful preliminary.

d. *The angular momentum problem*

Questions remain concerning the basic form of the terrestrial circulation. In particular, the *shape* of the eddies, their degree of regularity and mode of angular momentum transport constitute features that lack a *simple* explanation (Lorenz, 1967, 1969). This angular momentum problem relates to both the initial development of westerly jets by eddy action and the maintenance of existing jets by eddy interaction.

Various idealized eddy processes such as the baroclinic instability of meridionally sheared zonal flows (Pedlosky, 1964; McIntyre, 1970b; Williams, 1971) or vortex partitioning (Kuo, 1951, 1953) can yield some of the appropriate momentum characteristics. However, the different models reproduce these features for different reasons, so doubts exist as to whether the models relate to the atmospheric processes or describe coincidental effects. Any success of these eddy representations in circulation models (e.g., Charney, 1959) can be attributed to the inhibition of eddy growth by the strong surface drag.

e. *Current developments*

The description of the terrestrial circulation in terms of zonal means and eddies, with its simplistic dichotomy of scales and limited dynamics, is giving way to a more satisfactory view of the circulation in terms of the full spectrum of motion. This change has arisen from the appreciation of the relevance of the ideas of two-dimensional turbulence and nonlinear wave theory to atmospheric flow (see Section 4). These concepts also allow us to view the various circulations of the ocean, atmosphere and Jovian planets as manifestations of the same basic universal processes acting under different constraints; such a unification has long been regarded (Smagorinsky, 1969) as a desirable development in circulation theory.

4. Planetary turbulence and waves

Although recent studies emphasize the need to understand the complete spectrum of motion it is still convenient to subdivide the continuum into areas characterized by some specific property: on the smaller scale the ideas of two-dimensional turbulence prevail; on the larger scale, nonlinear wave theory; while at an intermediate scale k_β^{-1} both processes are equally active and form a third dynamical domain. In describing these dynamical regimes, we see characteristics that help explain Jovian behavior.

a. $k > k_\beta$: *Two-dimensional turbulence*

As a result of the conservation of enstrophy and kinetic energy (constraints unique to two-dimensional motion) kinetic energy is transferred to smaller wavenumbers where it is conserved, while enstrophy cascades to larger wavenumbers where it can be dissipated (Onsager, 1949; Fjortoft, 1953; Lilly, 1972; Bretherton and Haidvogel, 1976). If U is a typical velocity and L the dominant scale of energy containing eddies, then during the nonuniform evolution U remains approximately constant but L increases with time as the eddies coalesce into larger ones at a rate $\tau\sim UL^{-1}$ (Batchelor, 1969). So while the flow becomes larger in scale and smoother, the vorticity developes a finer structure. The spectral peak so dominates two-dimensional cascades that flow features can be specified by this single set of scales, a possibility unavailable in

three-dimensional motion and a property normally associated with linear processes only.

Whereas energy decay in three-dimensional turbulence has a time scale of UL^{-1} (determined by nonlinear exchanges), the much lengthier viscosity and a drag time scales L^2/ν and τ_D operate in the two-dimensional case. Thus the presence of strong eddies does not mean that energy dissipation is occurring; in fact, it is the distinct inability of two-dimensional turbulence to dissipate kinetic energy that is responsible for the preservation of the Jovian circulation and longevity of the Jovian disturbances.

In the limit of a purely two-dimensional cascade, energy accumulates at the lowest possible wavenumber, i.e., eddies grow to the size of the domain. Such an end state does not occur when surface drag (Lilly, 1972) or planetary wave propagation (Rhines, 1975) also operate. On Jupiter, drag effects must be weak so the cascade is more strongly modified by the more subtle Rossby-wave blocking effect.

b. $k \sim k_\beta$: *The Rhines effect*

On a rotating planet, the two-dimensional turbulent eddies—by expanding in size—become prone to the restoring effects of β, so the cascade eventually switches to a state of Rossby wave propagation. The time scale for the nonlinear interactions is $(kU)^{-1}$, where k^{-1} is the eddy diameter and U the rms particle speed. For Rossby waves of average orientation, the time scale is $2k/\beta$. The dynamical transition occurs where the two time scales become equal, when

$$k_\beta^2 = \beta/2U \tag{6}$$

(Rhines, 1973).

In the turbulent regime, the energy cascade to *smaller* k is also a migration to *smaller* frequency ω, for the relation $\omega \sim k|U|$ holds for the advective time scale. For the Rossby wave regime, the dispersion relation

$$\omega = \frac{-\beta}{k_1(1+k_2^2/k_1^2)}, \tag{7}$$

indicates an association of *smaller* frequencies with *larger* wavenumbers [for waves of the form $e^{(ikr-\omega t)}$, where k_1, k_2 are the longitudinal and latitudinal wavenumbers]. Thus, the ω, k relations of the turbulent cascade and wave propagation conflict at k_β, to the extent that the turbulent decascade of energy to smaller k nearly ceases—it is reduced by an order of magnitude (Rhines, 1975) for $k < k_\beta$—as the transition to wave motion occurs. Further spectral migration is slow so that k_β *remains the dominant scale* for considerable time. This wave-turbulence interaction and its properties will be referred to as the "Rhines effect" for convenience.

The blocking of the energy decascade by the wave regime does not proceed uniformly because of the anisotropic form of the dispersion relation. The turbulent cascade can proceed further if $k_2/k_1 \ll 1$, and the fluid achieves this by favoring the production of longitudinally oriented eddies, waves and currents. The transfer of energy to the zonal flow component and the production of an end state of the cascade in the form of alternating east–west zonal currents of scale k_β^{-1} was conjectured by Rhines (1975) and demonstrated by Williams (1975a,b). Our numerical solutions support the hypothesis that this production of zonal flow by the Rhines effect is responsible for the Jovian band structure and for zonality in the terrestrial circulation.

c. $k < k_\beta$: *Planetary waves and zonal flow*

The energy decascade is completed within the wave regime, $k < k_\beta$, with the formation of zonal currents. These can be shown to be barotropically stable (Rhines, 1975) under the integral stability condition $(f+\zeta)_y \neq 0$; however, the second stability criterion $\bar{u}(f+\zeta)_y > 0$, (e.g., Pedlosky, 1964) cannot be evaluated with comparable generality.

Spectral evolution and the stability of more complex flow configurations can be analyzed by nonlinear wave theory (e.g., Lorenz, 1972; Gill 1974). Weak nonlinear wave interactions can generate zonal flows under certain circumstances: (i) by a triad of Rossby waves when the meridional domain is finite and quantasizes the wave spectrum (Loesch, 1977); (ii) by a wave quartet in an unlimited domain (Newell, 1969; Loesch, 1977); and (iii) by side-band resonances of triads of continuous Rossby-wave packets (Newell, 1969).

Although zonal flow is a likely end state in atmospheric cascades, the theoretical understanding of its formation and maintenance remains rudimentary.

d. $k_z = 0$: *Barotropy*

The ideas of two-dimensional turbulence apply only to the barotropic component of motion, so the question that arises is under what circumstances, and to what extent, do baroclinic atmospheres behave in a barotropic or quasi-barotropic manner? The formal partitioning of energetics into barotropic and baroclinic components produces a complex system of interactions (Smagorinsky, 1963) that defies simple interpretation. Nonetheless, some empirical results (in addition to Kuo's) have been attained. In particular, a limited correspondence between barotropic and baroclinic states has been defined by the so-called equivalent barotropic model (Charney, 1949); a strong tendency toward barotropy in tropical regions devoid of moisture has been identified (Charney, 1963), and even in the ocean—where motions are strongest in a shallow layer above the thermocline—uniform barotropic models are relevant (Longuet-Higgins, 1965).

Further progress in resolving this issue has come from the cascade analysis of numerical solutions of freely evolving turbulence in the simpler quasi-

geostrophic models (Rhines, 1977). These solutions show that an initial baroclinic eddy field will in general evolve baroclinically, with decreasing vertical shear, until the eddy size reaches the deformation radius k_ρ^{-1}. Then follows a mutation to a barotropic state and a growth of eddies towards the k_β^{-1} scale, as discussed earlier. Thus quasi-barotropy may exist for $k<k_\rho$.

[Geostrophic turbulence (Charney, 1971) ignores the β effect and applies only to the $k>k_\rho\gg k_\beta$ range of scales.]

e. *Planetary regimes*

A similarity in nondimensional parameter values indicates a dynamical affinity between Jupiter and the ocean; thus, the turbulence concepts discussed above could also apply to the Jovian circulation. Estimates of the Jovian radius of deformation (1000–5000 km) are compatible with the existence of relatively small eddies which, as in the ocean, occupy $O(10^{-2})$ of the domain. Low values of the Rossby number suggest that Jupiter may have little or no tropical regime, being geostrophic to within 2° of the equator, as the ocean, rather than to within 30°, as the atmosphere.

Baroclinic instability probably operates sporadically and nonuniformly in its maintenance of the eddy fields of all three systems. Zonal momentum increases occur only every 10 days in the atmosphere and every few hundred days on Jupiter so exchanges may also be barotropic or quasi-barotropic on occasion.

The absence of efficient turbulent damping of the larger atmospheric eddies is a primary feature of terrestrial meteorology and can be accredited to the geostrophic nature of the flow. Yet the atmosphere, whose Ekman layer extends over one-tenth of the troposphere with a time scale of 5 days, must be characterized as strongly dissipative in comparison with the ocean, whose surface layer only extends over 1/500 of the depth with a dissipative time scale of the order of 500 days.

Two-dimensional turbulence models have been applied to the terrestrial atmosphere to try to explain the steep spectral slope observed at wavenumbers larger than $k_\rho=7$. Atmospheric spectra tend to be flat for $k<5$ (Leith, 1971), and this can be attributed to either the strong damping of surface drag (Lilly, 1972) or to blocking by the Rhines effect; a drag length scale $L_D\equiv U\tau_D=10^4$ km and a Rhines wavenumber of $k_\beta=4$ indicate that both processes are significant. The oceanic spectrum remains steep on the largest scales, so no energy can be cascading out of the large oceanic gyres.

Certain features observed in the Jovian and oceanic eddies imply the operation of the dynamics of β-modified two-dimensional turbulence. In Fig. 1 the smallest resolvable scale does not dominate the eddy size. The presence of distinctive scales suggests a wave dynamics and the sharp patterns and habitual longevity of the eddies reflect the inability of a two-dimensional flow to cascade energy to smaller scales.

The only simple calculation we can make for Jupiter involves evaluating the Rhines eddy radius $L_\beta=\pi k_\beta^{-1}$ in correspondence with the widths of the jet streams. For equatorial and midlatitude rms values of U of 100 and 20 m s^{-1}, L_β has values of 2×10^4 and 1×10^4 km, respectively.[4] These estimates plus their latitudinal variation agree with observation. The broader Saturnian bands are consistent with the higher velocities believed to be present in that atmosphere. For the Earth with $U=20$ m s^{-1} and $\beta=1.6\times10^{-8}$ km^{-1} s^{-1}, $L_\beta=4500$ km gives a reasonable estimate of jet width, despite the complexity caused by strong surface drag.

The precise length scale L_β should not be confused with the quantity $(U/\beta)^{\frac{1}{2}}$ that arises in scale analysis of the planetary vorticity equation (e.g., Batchelor, 1967); the former (latitudinal) length scale derives from a balance of nonlinear and linear terms, whereas the simple (longitudinal) length scale usually occurs for linear processes. Long (1961) and Hide (1969) have related the simpler scale to the width of the Jovian equatorial jet but with no physical rationale given. Barotropy and the scale $(U/\beta)^{\frac{1}{2}}$ were first involved in the Jovian context for a linear process, Rayleigh shear instability, by Haurwitz (1949) and later for one of the two barotropic stability criteria (Hess and Panofsky, 1951; Ingersoll and Cuzzi, 1969).

In summary, two regimes of planetary circulation can be discerned among the three systems. These can be characterized 1) for the Earth's atmosphere, as strongly dissipative (at the surface) with moderate β effects, i.e., $k_\beta\approx k_\rho\approx k_D$; and 2) for the ocean and Jupiter, as weakly dissipative with strong β effects, i.e., $k_D\ll k_\beta<k_\rho$. Although Jupiter provides the simpler example of the second regime, a separate polar state may exist on that planet. The cause of this may lie in the weakness of the eddy energy supply and in the exponential, rather than periodic, form of Rossby waves in high latitudes—both factors could prevent the completion of the wave-turbulence interaction.

5. Singular solutions

In contrast to describing the global circulation (Sections 3 and 4) specific solutions can be constructed for examining local aspects of the system, e.g., vortex shapes (Great Red Spot). Such solutions have value only if their functioning within the total scheme is known. The two major categories of restricted solutions involve steady state and steady wave approximations.

a. *Steady-state solutions*

The necessary and sufficient condition for permanent horizontal motion requires that the barotropic vorticity equation have solutions in which the absolute vorticity

[4] $\beta=0.5\times10^{-8}$, 0.36×10^{-8} km^{-1} s^{-1}.

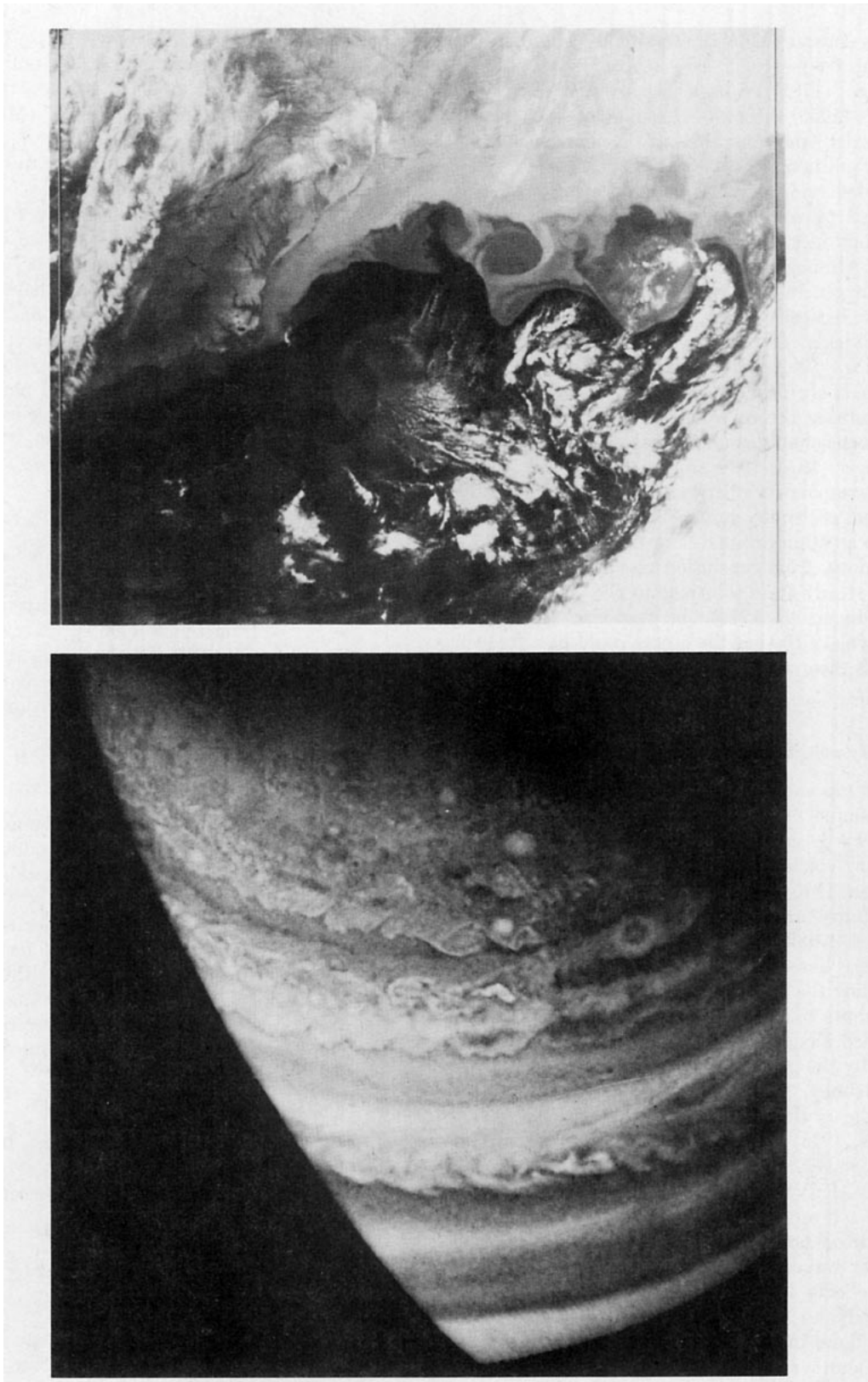

FIG. 1. Comparison of oceanic and Jovian eddies and waves. Top: Sea surface temperature patterns in the Gulf Stream near Cape Hatteras. Darker areas are warm. Courtesy R. Legeckis, National Environmental Satellite Service of NOAA. Bottom: Northern latitude cloud patterns on Jupiter. Courtesy of T. Gehrels, Pioneer II, NASA photograph.

remains constant along a streamline. The first-integral solution, $\zeta+f=Q(\psi)$, for such flows was noted by Lagrange (1781), Stokes (1842) and Ertel (1943). Arnold's (1965) theorem—that if $dQ/d\psi>0$, then stable states exist—provides the only general result for this form of solution.

The behavior of this class of solutions has been examined by selecting specific forms for the function $Q(\psi)$; but in practical problems $Q(\psi)$ is usually unknown. Although steady-state solutions should be nonlinear in general, the specific forms usually taken for $Q(\psi)$ are basically linear. The simplest case, $Q(\psi)$ constant, yields elliptical vortices when $\beta=0$ (e.g., Batchelor, 1967) and modified ellipses when $\beta\neq0$ (Godske *et al.*, 1957).

Concerning the relevance of $Q(\psi)$ type solutions to two-dimensional turbulence cascades, Bretherton and Haidvogel (1976) have shown that, when $\beta\neq0$, there is no correspondence between the respective steady and minimum enstrophy states. Thus $Q(\psi)$ solutions do not provide an appropriate description of turbulent β plane circulations. This conclusion also negates the application of steady-state solutions to the Jovian Great Red Spot (Ingersoll, 1973), in response to suggestions (Golitsyn, 1970) that the object could be a free vortex. Arnold's theorem indicates that these solutions are also unstable.

b. *Steady nonlinear waves*

Superimposable, permanent wave solutions, governed by a simple extension of steady-state integral solutions—$\Psi=\psi+cy$, $\zeta+f=Q[\Psi(x-ct, y)]$—exist for the planetary vorticity equation (Ertel, 1943; Craig, 1945; Neamtan, 1946), where c is the wave speed. Their superimposability arises from a choice of $Q=-k^2\Psi$ that yields essentially linear equations (Thompson, 1948). Analogous baroclinic solutions (Kuo, 1959) yield eddies resembling the model Jovian ones.

Attempts to deal with real wave nonlinearity have proceeded along two quite separate paths, determined purely by the magnitudes of geometrical wave parameters (Benney, 1971): one set contains the triad resonance theory that relates to two-dimensional turbulence (Rhines, 1975); the other produces a special class of steady waves, solitons, described by the Korteweg-DeVries (KdV) equation. In the physics of the KdV scheme a mean flow supports a *small* wave that gives rise to *small* nonlinear effects that are *weakly* dispersed by other waves. In the turbulence scheme *large* nonlinear effects lead to *steep* waves that are *strongly* dispersed and feed energy into the mean flow. The energy flows in the two schemes are directly opposed to one another so the dynamics of the KdV equation does not relate to two-dimensional turbulence.

The original planetary solitons obtained by Long (1964), for a zonal flow with a weak uniform shear, were oval in form—the meridional shear is necessary for soliton existence (Benney, 1966; Clarke, 1971). More complex mean flows, e.g., $\bar{u}\approx\tanh y$, yield more complex forms, e.g., modified ellipses, that have been equated with the Great Red Spot (Maxworthy and Redekopp, 1976a,b).

As a model of the Great Red Spot the soliton theory has serious limitations: 1) the stability characteristics of multiple-jet flows differ considerably from those of a single jet (Haltiner and Song, 1962) so reevaluation is necessary; 2) the meridional length scales [dependent on $\bar{u}(y)$] are considerably smaller than L_β or the observed vortex; 3) the one-dimensional (longitudinal) KdV equation cannot explain meridional uniqueness; 4) the physical relevance of the KdV equation, with its special balance of weak but matched phase and amplitude dispersions, requires a remarkable form of stability that is difficult to justify (Benjamin, 1974)—particularly for a turbulent atmosphere.

c. *Jovian gyres*

Closed contours in the absolute vorticity field normally characterize a turbulent regime, open contours a wave regime. Jovian gyres, by their proximity in size to the transitional scale k_β^{-1}, are complex intermediate phenomena. Although ellipses and ovals appear to be the preferred eddy shapes in many quasi-linear models, the assumptions behind their formation remain speculative.

6. Forced barotropic model

We begin our numerical studies by examining those quasi-barotropic responses that produce circulations with large-scale flow features comparable to those of the terrestrial and Jovian atmospheres. We are particularly interested in isolating and understanding mechanisms that produce zonality and jet formation and in defining their relationship to the Rhines and Kuo processes. To achieve the appropriate motions, a quasi-barotropic model with an implicit representation of baroclinic forcing effects will be formulated.

a. *Equations*

The two-dimensional, nondivergent, barotropic vorticity equation for fluid motion on a rotating sphere (e.g., Silberman, 1954) may be written in the form

$$\zeta_t+\psi_x(\zeta+f)_y-\psi_y\zeta_x=\nu\nabla^2\zeta+F-D, \tag{8}$$

$$\zeta=m^2\psi_{xx}+(m^{-2}\psi_y)_y, \tag{9}$$

where

x	prograde longitudinal coordinate $[=a\phi]$
y	northward latitudinal coordinate $[=a\sin\theta]$
a	planetary radius
(θ,ϕ)	latitude, longitude
m	$\sec\theta$, a mapping factor
β	northward gradient of Coriolis term $[=2\Omega/am]$

f Coriolis term $[=2\Omega y/a]$
ζ vertical vorticity component $[=mv_x-(u/m)_y]$
(u,v) velocities in (x,y) directions $[=-\psi_y/m, m\psi_x]$
∇^2 Laplacian operator $\{=m^2(\ )_{xx}+[(\ )_y/m^2]_y\}$
ν horizontal mixing coefficient
F forcing term
τ_D time scale of Ekman drag
D surface drag $(D_1=\zeta/\tau_D, D_2=\zeta\sin\theta^{\frac{1}{2}}/\tau_D)$.

The coordinates defined above were selected because of their suitability for finite-difference calculations in the spherical domain. In particular, they produce equal area grids, efficient in polar regions, and lead to advection Jacobians suited to the Arakawa (1966) difference forms. The energy- and enstrophy-conserving properties of the latter are essential for the accurate and stable simulation of turbulent flows. The Appendix contains details of the numerical scheme.

b. *Boundary conditions*

Integrations were made for various global sectors, with periodic boundaries at longitudes $\phi=0$, Φ, and with impermeable boundaries, $v=\psi'=0$, at latitudes $\theta=\theta_-,\theta_+$.

The following problems exist in selecting the most appropriate lateral boundary conditions for the finite-difference equations: 1) truncation errors (at the walls) between the ψ,ζ variables prevent the definition (to second-order accuracy) of the Poisson equation for the $\bar{\psi}$ component and of a unique $\bar{u}$ value; 2) to fulfil the conservation properties of the Arakawa Jacobian the ζ_t equation must be used at the sidewalls—this excludes use of a physical slip condition $\zeta_B=0$ (where the subscript B denotes boundary values); and 3) specific interest in high-Reynolds' number flow suggests the desirability of a numerical scheme that, on taking the limit $\nu=0$, yields the preferred inviscid flow method.

In designing boundary conditions, constraints on the global angular momentum can only be approached implicitly through integrals relating it to the basic variables ψ,ζ. These are

$$\int m\bar{u}dy=\bar{\psi}(\theta_-)-\bar{\psi}(\theta_+), \tag{10}$$

$$\int\bar{\xi}dy=\bar{M}_{\theta_-}-\bar{M}_{\theta_+}, \tag{11}$$

$$\int\tilde{y}\bar{\xi}dy=\bar{\psi}(\theta_-)-\bar{\psi}(\theta_+)-[\tilde{y}\bar{M}]_{\theta_-}^{\theta_+}, \tag{12}$$

where $M=-\psi_y/m^2$ is a measure of the angular momentum ($\bar{\xi}=-\bar{M}_y$) and $(^-)$ denotes the zonal mean. The weighting function

$$\tilde{y}(y)=\int_{\theta_-}^{\theta}m^2dy$$

reduces to y in the β plane approximation. Eqs. (11) and (12) cannot be realized in the finite-difference domain, due to the indefineable (to second-order accuracy) ψ_y boundary terms. Thus the angular momentum constraint inherent in Eq. (12) cannot be achieved exactly.

The need to prevent the artificial sidewalls from contributing to the angular momentum and vorticity of the flow requires that computational, rather than physical, conditions be imposed. Thus, we attain a state of *wall-neutrality* by setting $\nu\zeta_y=0$ in the ζ_t equation on the sidewalls, to guarantee vorticity integrity, and by using one of the following conditions on $\bar{\psi}_B$ for the Poisson equation to try to conserve global angular momentum:

BOUNDARY CONDITION 1 (BC1): $\bar{\psi}_B=0$.

BOUNDARY CONDITION 2 (BC2): $\bar{\psi}_t(\theta_+)-\bar{\psi}_t(\theta_-)=-\int_{\theta_-}^{\theta_+}\tilde{y}\bar{\xi}_t dy$.

BOUNDARY CONDITION 3 (BC3): $\bar{\psi}_y=0$, defined using Eq. (11)—see Appendix.

The second condition allows $\bar{\psi}_B$ to be predicted and it conserves global angular momentum to within the accuracy of the sidewall truncation errors. With the BC1 and BC3 schemes, global angular momentum is conserved to a tolerable level for the relatively short-term, weakly dissipative calculations. Solutions are relatively insensitive to the boundary condition scheme because of the dynamical insignificance of the constant $\bar{\psi}_B$ term.

c. *Dissipation and resolution*

The value of the viscosity coefficient ν is chosen in relation to the high numerical resolution ($\sim 128^2$) necessary for turbulence simulation. Optimum viscosity values exist at each resolution, being such as to produce a spectrum in which all scales of motion contributing to the enstrophy dissipation rate are resolved. Failure to use adequate viscosity or resolution leads to unrealistic solutions that display an equipartitioned spectrum, i.e., one in which energy is randomly and equally distributed in all modes.

The viscosity resolution requirement is achieved by examining flow spectra and by monitoring a macroscopic turbulent Reynolds number

$$R_T=\tfrac{1}{2}\overline{u^2}/\nu\eta^{\frac{1}{3}}, \tag{13}$$

where $\eta=-\overline{\nu\zeta\nabla^2\zeta}$ is the enstrophy dissipation rate. Smaller scales become less accurately treated as R_T increases in a fixed resolution calculation. However,

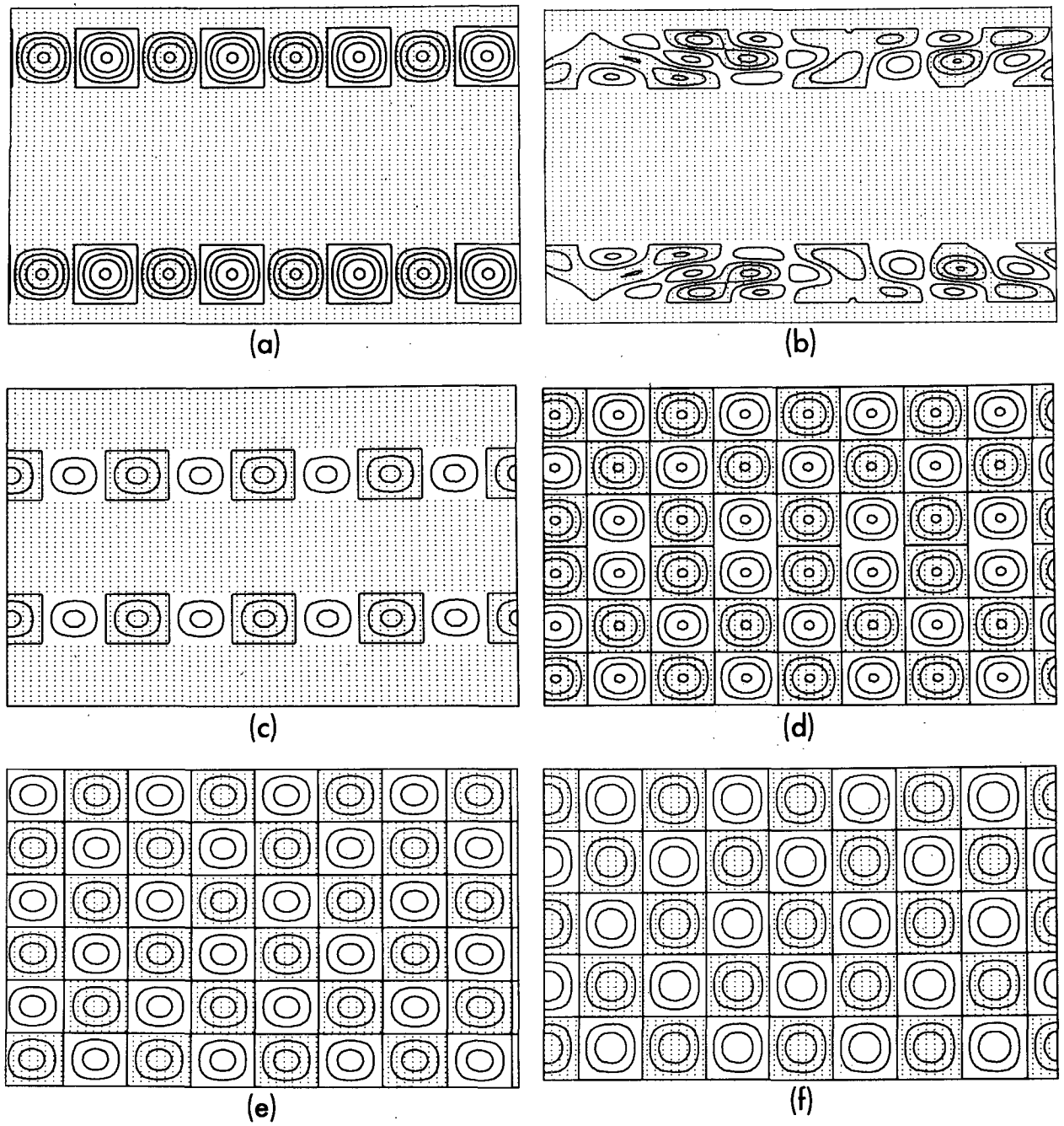

FIG. 2. Examples of random phase stochastic forcing fields F used in cases E1–E7. Vertical axis is y coordinate from $\theta = -80°$, 80°. Horizontal axis is longitude over 180°. Contours are shaded by selected grid points in regions where they are zero or negative.

(a) Case E1 and E3. Contour interval $\Delta F = 10^{-10}$ s^{-2}.
(b) Case E2. $\Delta F = 4\times10^{-10}$ s^{-2}.
(c) Case E4. $\Delta F = 2\times10^{-10}$ s^{-2}.
(d) Case E5. $\Delta F = 2\times10^{-10}$ s^{-2}.
(e) Case E6. $\Delta F = 2\times10^{-10}$ s^{-2}.
(f) Case E7. $\Delta F = 1\times10^{-10}$ s^{-2}.

large-scale features of the flow field remain essentially independent of the Reynolds number[5] and can be accurately represented at R_T values two or three times larger than the optimum values of 150, 350, 1100 that hold for resolutions of 64^2, 128^2, 256^2, respectively (Herring *et al.*, 1974). All calculations lie within this acceptable range of R_T values.

[5] This result allows changes in the ν value to be made during a calculation if necessary.

d. Forcing formulation

To sustain a turbulent flow and produce stationary solutions requires a forcing mechanism $F(\mathbf{r},t)$. The problem is to deduce what forms of F are most appropriate to the planetary circulations.

If in a baroclinic two-layer model, the stream-functions for the nondivergent flows in these layers are written as $\psi+\sigma$ and $\psi-\sigma$, then the governing equation for the barotropic component can be written (Lorenz, 1962)

$$\nabla^2\psi_t+J(\psi,\nabla^2\psi+f) = -J(\sigma,\nabla^2\sigma)-\frac{\nabla^2\psi}{\tau_D}+\frac{\nabla^2\sigma}{\tau_D}+\nu\nabla^4\psi. \quad (14)$$

To represent baroclinic flows as forced barotropic ones requires that F be chosen to imitate the baroclinic Jacobian term $J(\sigma,\nabla^2\sigma)$ and also in strong drag cases to take account of the baroclinic drag component $\nabla^2\sigma/\tau_D$. This problem is related to that of turbulence theory where approximations and closure schemes are designed to represent such nonlinear interactions. Unlike turbulence theory, however, we deal with the *barotropic* nonlinear terms in toto and parameterize only the baroclinic component.

The stochastic treatment of nonlinear interactions has shown that phase relations among individual spectral components become increasingly random (Kraichnan, 1958, 1961), that this random coupling can be described by simple Markovian models (Leith, 1971; Kraichnan, 1971; Frisch *et al.*, 1974), and that randomly fluctuating forcing functions can maintain such exchanges (Edwards, 1964). This suggests that a Markovian random forcing formulation for $F(\mathbf{r},t)$ could provide a reasonable representation of the baroclinic Jacobian term. In this way the forced baroclinic model can be made to provide a probabalistic analog of the deterministic atmospheres. This stochastic approach to meteorological questions dates back to Lorenz (1953), with significant contributions by Epstein (1969) and Mak (1969).

Simple turbulent states can occur when the forcing is defined by the Langevin equation (e.g., Yaglom, 1962), the most elementary Markovian process with space and time variation, i.e.,

$$\frac{\partial F}{\partial t}=-\frac{F}{\tau_F}+\frac{\hat{F}}{\hat{\tau}_F}. \quad (15)$$

This equation provides a model for such statistical physics problems as Brownian motion (Chandrasekhar, 1943). For finite-difference calculations this equation can be written (Lilly, 1969), for F at time step n, as

$$F_n=R_nF_{n-1}+(1-R_n^2)^{\frac{1}{2}}\hat{F}_n, \quad (16)$$

where $R_n\equiv(1-\Delta t/2\tau_F)/(1+\Delta t/2\tau_F)$ is a dimensionless (memory) coefficient, $\hat{F}_n$ the random modifier of F_n and τ_F the autocorrelation time-scale of the random sequence. Specifying a time-scale $\hat{\tau}_F=(\tau_F\Delta t/2)^{\frac{1}{2}}$ produces the simple form of (16), where Δt is the time step.

The source function $\hat{F}_n$ is generated by selecting (normalized) random coefficients for a Fourier mode representation

$$\hat{F}=\sum_{\boldsymbol{\kappa}}\hat{F}_{\mathbf{k}}\exp(i\mathbf{kr})$$

that has wavenumbers $\mathbf{k}$ restricted to those $\boldsymbol{\kappa}$ lying on a rectangular, rather than a circular surface, in wavenumber space. This specification allows for the anisotropic atmospheric situation where the predominant latitudinal and longitudinal wavenumbers κ_y, κ_x are determined by different dynamical processes: κ_x by the baroclinic radius of deformation and κ_y by combinations of the radius of deformation and the barotropic environment.[6] Terms capable of directly inducing mean or

[6] Specifying κ_y is a limitation of the forced barotropic model.

TABLE 1. Terrestrial barotropic calculations. Details of four locally and three globally forced flows: θ_F denotes region of forcing and κ_x, κ_y the wavenumber range of the forcing over the intergration domain. In case E4 , an auxiliary forcing function of amplitude 0.2×10^{-10} s^{-2} yields the westerly flow $u\sim(1-\cos\theta)$. R_T is a typical value of the turbulent Reynolds number and $\langle u\rangle$ the final rms velocity. Other parameters are $a=6360$ km, $\Omega=0.729\times10^{-4}$ s^{-1}, $\theta_-=-80°$, $\theta_+=80°$, $\Phi=180°$, $\tau_F=10^5$ s. Resolution is 128×128. Drag form D_1 used. BC denotes boundary condition scheme (see Section 6b).

Case	$\lvert\theta_F\rvert$	κ_x	κ_y	$\lvert F\rvert$ (10^{-9} s^{-2})	τ_D (10^5 s)	ν (km^2 s^{-1})	R_T	$\langle u\rangle$ (m s^{-1})	Δt (10^3 s)	BC	Characteristic
E1	30–60°	4	1	10	∞	0.1	400	26	6	BC1	Simple local forcing
E2	30–60°	3,5	1,3	6	∞	0.1	400	29	4	BC1	Complex local forcing
E3	30–60°	4	1	10	5	0.05	800	29	5	BC1	Simple local forcing with drag
E4	17–37°	4	1	10	5	0.1	300	22	5	BC2	Simple local forcing with mean flow and drag
E5	0–80°	4	3	6	∞	0.1	900	50	5	BC5	Symmetric global forcing
E6	−80–80°	4	3	8	∞	0.1	700	50	5	BC1	Asymmetric global forcing
E7	−80–80°	4	5	6	∞	0.1	700	42	5	BC1	Trans-equatorial global forcing

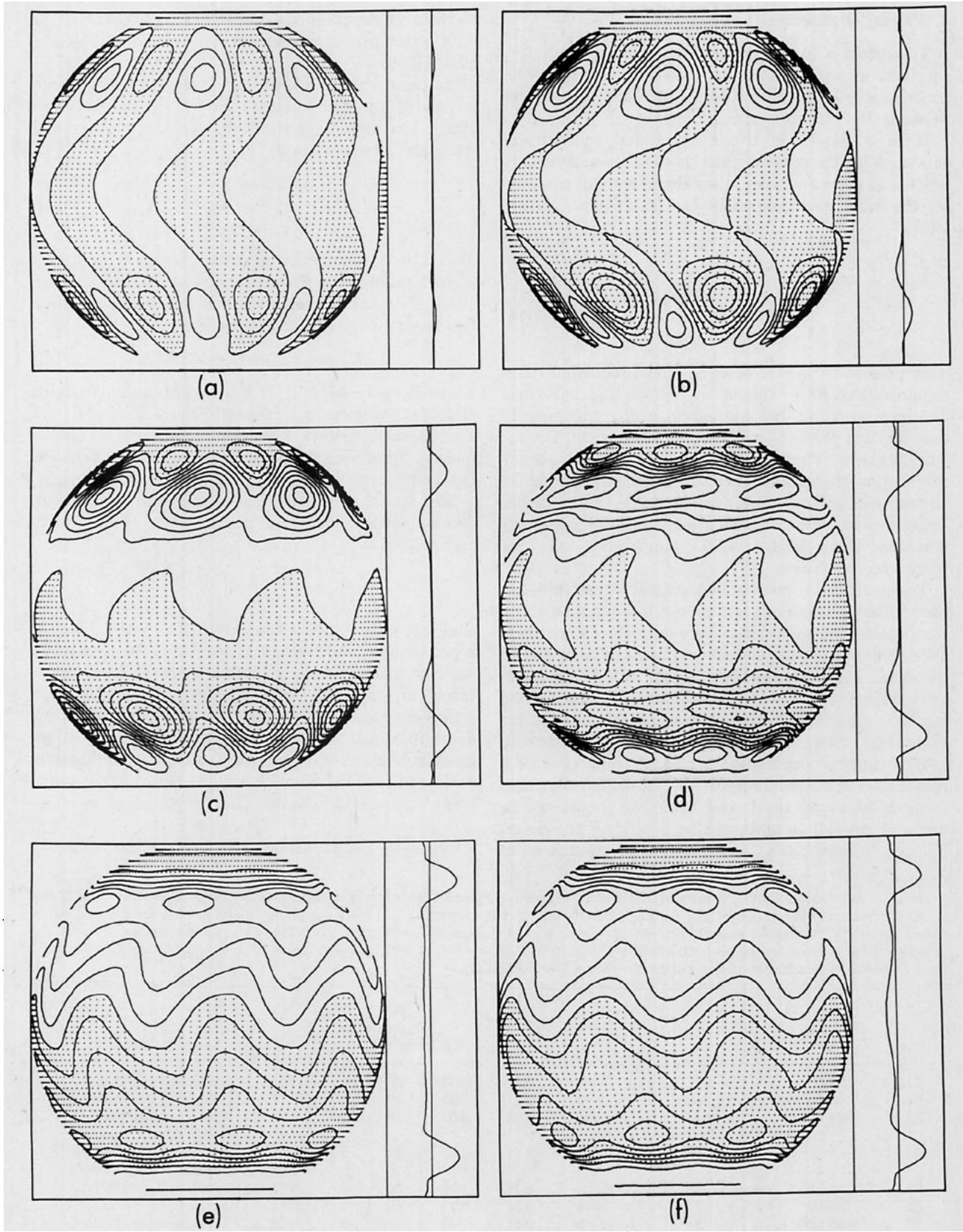

FIG. 3. Case E1 streamfunction evolution. Midlatitude forcing, contour interval (a)–(d) $\Delta\psi = 10$ km^2 s^{-1}, (e)–(l) $\Delta\psi = 15$ km^2 s^{-1}. Corresponding mean zonal flow on right-hand side has scale $\pm u^* = 100$ m s^{-1}, zero value at center line. Spherical projection has longitudinal positions for abscissa $x' = a(1-\cos\theta\cos\phi)$ and ordinate $y' = a\sin\theta$. Negative function values are shaded by selected grid points.

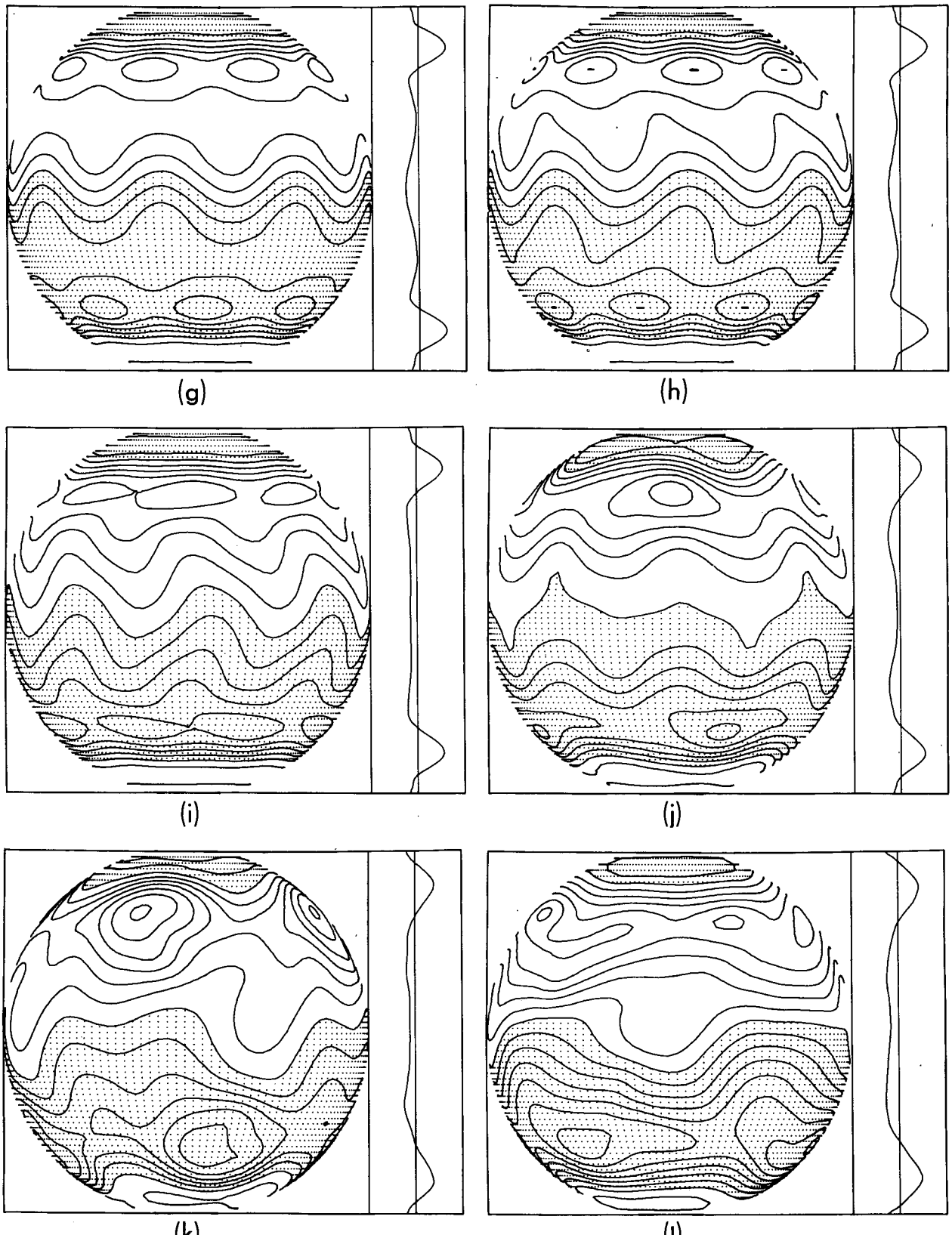

Same notation in all figures. Streamfunction and $\bar{u}$ shown at days (a) 4.1, (b) 5.5, (c) 6.2, (d) 6.9, (e) 10.3, (f) 11.7, (g) 13.1, (h) 14.4, (i) 16.5, (j) 18.6, (k) 20.7, (l) 31.0.

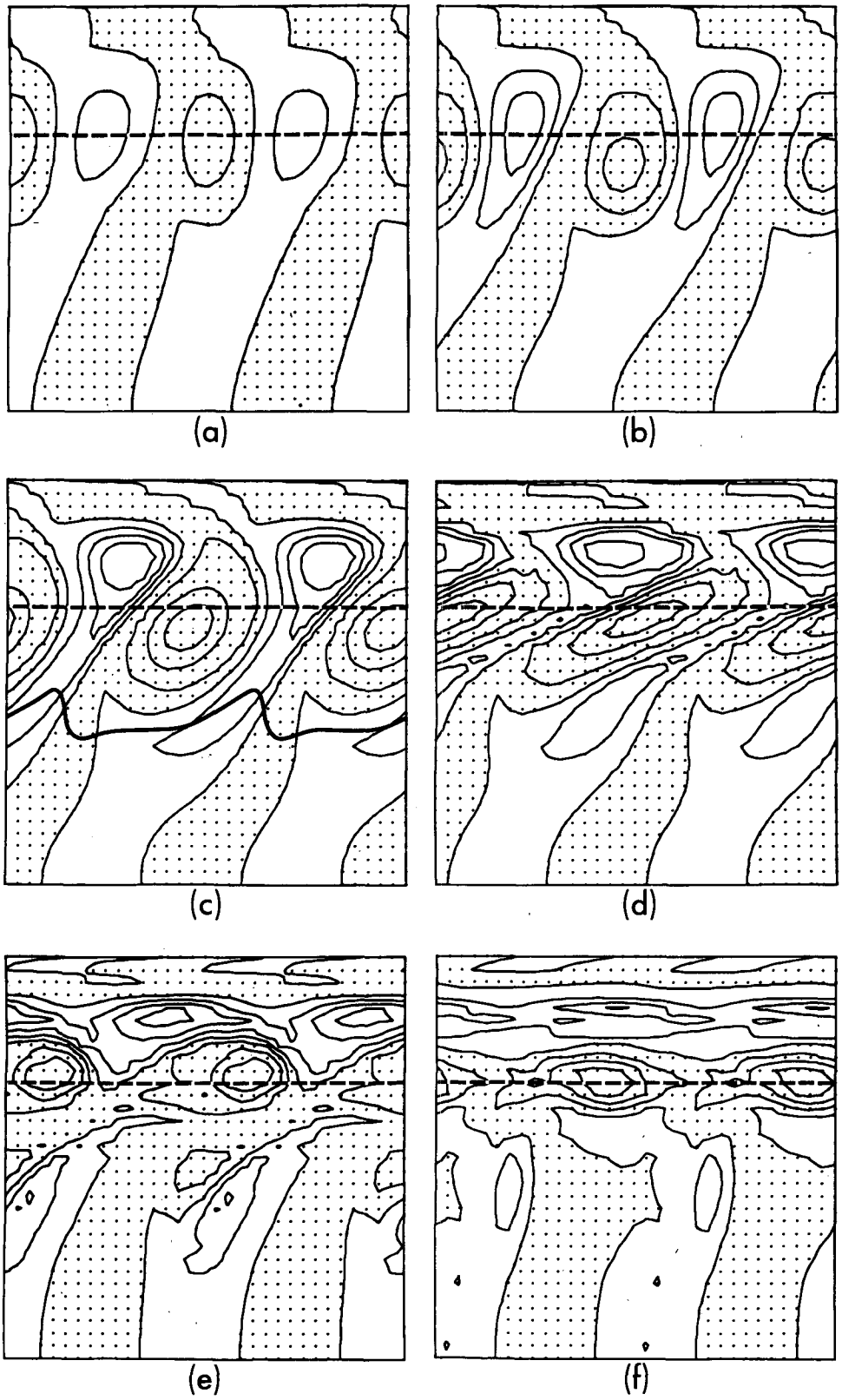

FIG. 4. Case E1, vorticity evolution. Contour interval $\Delta\zeta = 4\times10^{-5}$ s^{-1}. Negative values are shaded by selected grid points. Coordinates are $x' = x$, $y' = a\sin\theta$. Domain is one-fourth of integration region: $\theta = 0, 80°$, $\phi = 90, 180°$. Reference axis (dotted line) denotes middle of forcing zone and 4c has a stream-function contour superimposed. Vorticity is shown at days (a) 3.4, (b) 4.8, (c) 6.2, (d) 6.9, (e) 8.2, (f) 10.3.

boundary flows are omitted, i.e., $\overline{\bar{F}}=0$. This type of forcing produces flows analogous to those created by mechanical or thermal processes that can stir the atmosphere at fixed κ and τ_F scales.

For Jovian studies, this type of forcing provides an ideal, minimally constrained set of assumptions about the source of energy. The calculations show that small values of κ most effectively produce realistic flows, and this leads us to regard F as a representation of baroclinic instability and not of convection, which would require a large value of κ. However, other interpretations are possible if alternative mechanisms, producing large eddy fields, can be discovered.

For the Earth, when F is constrained to zonal belts, vorticity concentrations can be produced in the form conceived by Kuo (1951) as depicting the operation of baroclinic instability.

7. Terrestrial solutions

The barotropic prediction equations (8), (9) and (16) were integrated with a variety of forcing configurations (Fig. 2) for terrestrial values of a and Ω. The selected sample of solutions (Table 1) illustrates the simplest conditions under which terrestrial circulations can occur, cases E1–E4, and some of the main alternative response forms, cases E5–E7. All calculations begin with a fluid at rest and use a viscosity value that gives as high a Reynolds number as is compatible with the resolution, in order to yield inviscid-type solutions rather than equilibrated flows.

a. E1: *The basic case—inhomogeneous forcing*

The vorticity forcing function in Fig. 2a provides a simple representation of the action of baroclinic eddies in midlatitudes. The forcing eddies randomly vary their longitudinal positions while fluctuating in amplitude below an upper limit, chosen to give a flow with velocity scale of 20 m s^{-1} in the first week.

The main steps in the formation of midlatitude westerlies and tropical easterlies are shown by the streamfunction field of Fig. 3, and in greater detail by the vorticity field of Fig. 4. To identify physical effects comparison is made with a solution obtained under similar conditions but with $\Omega=0$ (Figs. 6 and 7).

Although the initial flow development directly reflects the forcing through the production of matching cyclones and anticyclones[7] along the reference axis as shown in Figs. 3a and 4a, the fluid filters out the random phase behavior; as a result, the eddies do not move longitudinally.[8] The eddies act as a wave maker for the unforced zone where Rossby waves with the same wavenumber as the forcing set in. The westward propagation is most rapid at the equator due to the maximum value of β there. The differential wave propagation orients the phase lines (zero amplitude contours) westward from the reference axis.

The eddies strengthen under the persistent forcing, become deformed by nonlinearity and move north–south under the influence of β (Figs. 3b and 4b). The tendency for cyclones (anticyclones) to move poleward (equatorward) to latitudes of similar absolute vorticity, as predicted by Kuo (1951), initiates a poleward vorticity and momentum transfer. The alignment of eddies along a southwest-northeast axis by the β term produces the classical shape required for such transfers.

The onset of net final flows and continuous sets of cyclones and anticyclones mark the completion of vortex partitioning at 6.2 days (Fig. 3c). Eddy tilt increases, and significant shear layers form on the eastern side of the cyclones (Fig. 4c). Such concentrations are a feature of two-dimensional enstrophy cascades, but this anisotropic distribution can only be attributed to the simultaneous eddy motion and reorientation caused by the β effects. The superimposed ψ contour in Fig. 4c indicates the close relation between (momentum transferring) "sawtooth" streamfunction formations and vorticity shear layers.

The development and rapid cascade of energy into the zonal mode is caused by the initiation of Rossby wave propagation within the forced zone, an event that also activates the eastward propagation of the vortices (Figs. 3d and 4d). The flow after 7 days consists of a 60 m s^{-1} westerly jet in the higher (forced) latitudes balanced by a comparable easterly jet on the adjacent equatorward side. Following this buildup of midlatitude zonal currents, the flow enters a second phase (lasting two weeks) during which steep Rossby waves transfer the momentum of the easterly jet to the equator and back again (Figs. 3e–3l).

By 8.2 days, eddies of like sign have joined together, but their shear layers still retain a relation with the generation of momentum transferring tropical Rossby waves (Fig. 4e)—evidence in support of such a connection is provided by the simultaneous disappearance of shear layers and momentum transfer at later stages (Fig. 4f). The saw-toothed westerly propagating waves have the appropriate forms for transferring *easterly* momentum *equatorward*, or *westerly* momentum *poleward*, but the chain of events indicates that the former is occurring. By 10.3 days, sufficient easterly momentum has been transferred equatorward to create a 14

[7] The term cyclone (anticyclone) is used to denote regions in the Northern Hemisphere where ψ is a minimum (maximum) and ζ is a maximum (minimum) and vice versa in the Southern Hemisphere.

[8] This result (somewhat biased by having chosen a relatively small τ_F) suggests that the atmosphere's barotropic component may not respond to the more rapid baroclinic changes, just as the ocean fails to react to the higher frequencies of wind stress.

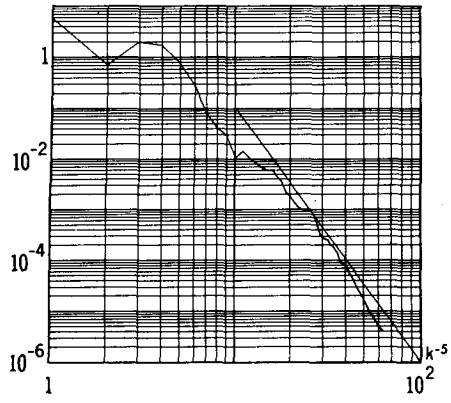

FIG. 5. Case E1, kinetic energy bispectrum at 31 days. Abscissa is wavenumber.

m s^{-1} uniform easterly flow, of the form predicted by Eq. (4) (Fig. 3e).

Momentum begins to accumulate at the equator (Fig. 3f) with a 28 m s^{-1} peak occurring at 13.1 days when the waves display a neutral form (Fig. 3g). As easterly momentum begins to return to midlatitudes, the mean zonal flow reverts to early forms—cf. Figs. 3e, 3f with 3h, 3i—but with the wave patterns reversed.

The returning energy eventually interacts with a midlatitude flow that has remained relatively constant. The exchange does not restore the original easterly jet, but instead puts energy into higher wavenumber components (Fig. 3j). This enhances the anticyclonic gyres to a maximum and makes the westerly jet undular (Fig. 3k). The circulation then becomes complex, and the further evolution cannot be deciphered easily. The final, partially equilibrated, configuration consists of a basic westerly–easterly zonal flow form (Fig. 3l). The discrete Rossby wave propagation at κ_x disappears as the spectrum fills in to a sharply peaked k^{-4} to k^{-5} form (Fig. 5).

b. E1: *Implication*

The solution described above provides an example of a simple nonlinear process that produces zonal flows in response to energy sources that are neither as simple as those of linear instability nor as chaotic as those of full turbulence. The flow scenario thus prompts the following (limited) explanation for the preferred atmospheric momentum characteristics, in response to the problem posed by Lorenz (1967, 1969). (see Section 3d).

Forcing effects (cyclogenesis) in midlatitudes create a set of cyclones and anticyclones within that zone. The behavior of these developing eddies is controlled by three β-related mechanisms and by the nonlinear two-dimensional cascade process. Flow development can be broken down into the following five stages:

1) As the eddies are created, the vortex partitioning process (the first β mechanism) moves them to latitudes with their own absolute vorticity and aligns them into a southwest-northeast configuration. This creates the easterly and westerly momentum zones and preferred eddy shapes.
2) The eddies generate *external* Rossby waves (the second β mechanism) in the unforced zone. These waves are initially weak but their differential phase propagation appears to reinforce the preferred eddy orientation.
3) Simultaneously, but more slowly, the enstrophy cascade creates vorticity shear layers and distorts the eddies. These anisotropic eddies make the *external* Rossby waves anisotropic and thence capable of transferring momentum equatorward.
4) The energy decascade generates and is retarded by *internal* (to the forced zone) Rossby waves (the third β mechanism), as in the Rhines effect. This interaction terminates eddy development and enhances the westerly jet.
5) The blocking by *internal* waves forces significant energy to go into the *external* waves, the latter only become strong after the establishment of a wave regime in the forced zone. This transfer creates the tropical easterlies and a more obvious westerly jet in midlatitudes.

The E1 circulation can be interpreted only partly in terms of the Kuo and Rhines effects. The presence of inhomogeneous forcing with a meridional scale $\kappa_y \approx k_\beta$ and the generation of separate sets of Rossby waves define a more complex phenomenon than the theories consider. Further resolution of the angular momentum problem requires a more penetrating analysis of such phenomena.

c. E1 *subcase:* $\Omega = 0$

To support our interpretation of the E1 solution, particularly as regards the role of β, the case was re-evaluated with Ω set to zero; the results are shown in Figs. 6 and 7. The development of the rotating and nonrotating flows diverges after 4 days. The enstrophy cascade controls the nonrotating flow to produce predominantly "cyclonic" eddies and an uneven vorticity clustering (Figs. 6a and 7a)—the eddies extend further latitudinally in the absence of β. The "cyclones" continue to strengthen, coalesce and transfer energy into the largest scales (Figs. 6b and 6c), while the vorticity elements move into the quiescent tropical region where they remain and decay (Figs. 7b–7d).

The resulting westerly and easterly zonal circulation should be regarded as a domain-sized eddy: the end product of a two-dimensional cascade energized by forcing with limited harmonic content. Such solutions may be relevant to the circulations of Venus and the Sun, but the forcing mechanism needs reinterpretation.

d. E2: *Complex inhomogeneous forcing*

To examine the sensitivity of the circulation to forcing composition, we consider the solution E2 produced by forcing with a richer component mix (Fig. 2b) than in the simple E1 state. Although the details of flow evolution differ from those of E1, the equilibrating circulation at one month, shown in Fig. 8, is very similar. Over the long term nonlinear barotropic exchanges fill out the spectrum, regardless of any baroclinic process (or its imitation) doing likewise. Thus, the simpler forcing form of E1 provides an adequate facsimile of baroclinic processes, justifying the single-mode forcing adhered to in the remaining examples.

e. E3: *Surface drag—inhomogeneous forcing*

In the atmosphere, surface drag and details of flow equilibration become important for time scales greater than a few days. Introducing a strong drag into the E1 scheme produces a circulation that differs from that of the non-drag case. Initially, westerly jet formation occurs in the forced zone but the easterly counterflow and anticyclones persist (Fig. 9a). Eventually, this configuration disintegrates into a flow with a final mean zonal flow similar to that of E1. However, energy remains in larger wavenumbers due to the blocking of the decascade by the drag and large gyres prevail.

f. E4: *Supplementary forcing*

The enigmatic result in E3—that under more realistic conditions the circulation becomes less realistic—can be attributed to the drag formulation. The baroclinicity of the atmosphere and the geostrophic constraint impart a vertical structure, to both mean flow and disturbances, resulting in a surface dissipation not easily represented by a one layer model. The issue can be resolved by allowing an implicit representation of the baroclinic drag component, $\nabla^2\sigma/\tau_D$ in Eq. (14), via a supplementary forcing function that produces the appropriate secondary flow component. This *baroclinic* drag term can inject energy into the barotropic flow at the largest scales of motion, thereby modifying the barotropic β drag blocking effects.

As an example, case E4 has an adjunct forcing that produces a simple westerly flow and a stochastic forcing centered about the peak of this flow (Fig. 2c)—both forcing components have amplitudes that yield comparable flow maxima. Together, the forcing fields produce a stable, predominantly zonal flow configuration, consisting of weak tropical easterlies and a westerly jet with a maximum poleward of the forcing axis.

g. Global forcing

Having reproduced terrestrial-type circulations for a situation with known forcing, we must now consider more general response properties, to cover circumstances where the forcing must be implicitly inferred. For convenience, only one class of solutions will be presented: that produced by simple homogeneous eddy forcing fields whose interhemispheric symmetry varies. Emphasis is on initial development, not equilibrium, and flow configuration is conditional on amplitude. At higher energy levels k_β tends to zero and flows take on an alternative, less zonal climatic form.

h. E5: *Symmetric global forcing*

Forcing that is symmetric about the equator (Fig. 2f) produces a circulation with a distinctive equatorial jet of 100 m s^{-1} and a broad midlatitude easterly belt (Fig. 11). The vorticity field exhibits the cross-equatorial wave mode that maintains the equatorial jet. As in cases E1–E4, the dominance of wave propagation means that the vorticity field displays little of the fine-structure associated with two-dimensional turbulence cascades.

i. E6: *Asymmetric global forcing*

Equatorially asymmetric forcing (Fig. 2e) produces a circulation with tropical westerlies and midlatitude easterlies as shown in Fig. 12a. However, the westerly current does not have a distinctive jet form, as is reflected in the absence of a cross equatorial vorticity transfer in Fig. 12b—and its decline right at the equator indicates that the flow is produced in the zone near the equator, not at it.

j. E7: *Cross-equatorial global forcing*

For transequatorial forcing (Fig. 2f), the mean circulation in Fig. 13 has a smooth oscillatory variation in latitude. Equatorial westerlies occur again in response to the cross-equatorial vorticity transfer. The three westerly and two easterly jets are very similar to each other in magnitude and form and are separated by large rotating gyres.

Unlike the locally forced flows, which can be understood using the ideas of Kuo (1951), the development of globally forced circulations can only be described in terms of the less specific Rhines effect. Although alternating east–west flow appears to be the universal characteristic, the correlation between the forcing zones and flow remains obscure. The ease with which equatorial westerly jets can be produced by hemispherically symmetric forcing is of significance for various astrophysical problems, the full solution of which needs only the identification of an appropriate vorticity source.

8. Jovian solutions

The main difficulty in applying the forced barotropic model to the Jovian atmosphere lies in estimating the scale and distribution of the driving and the character of the underlying surface. We have opted for the

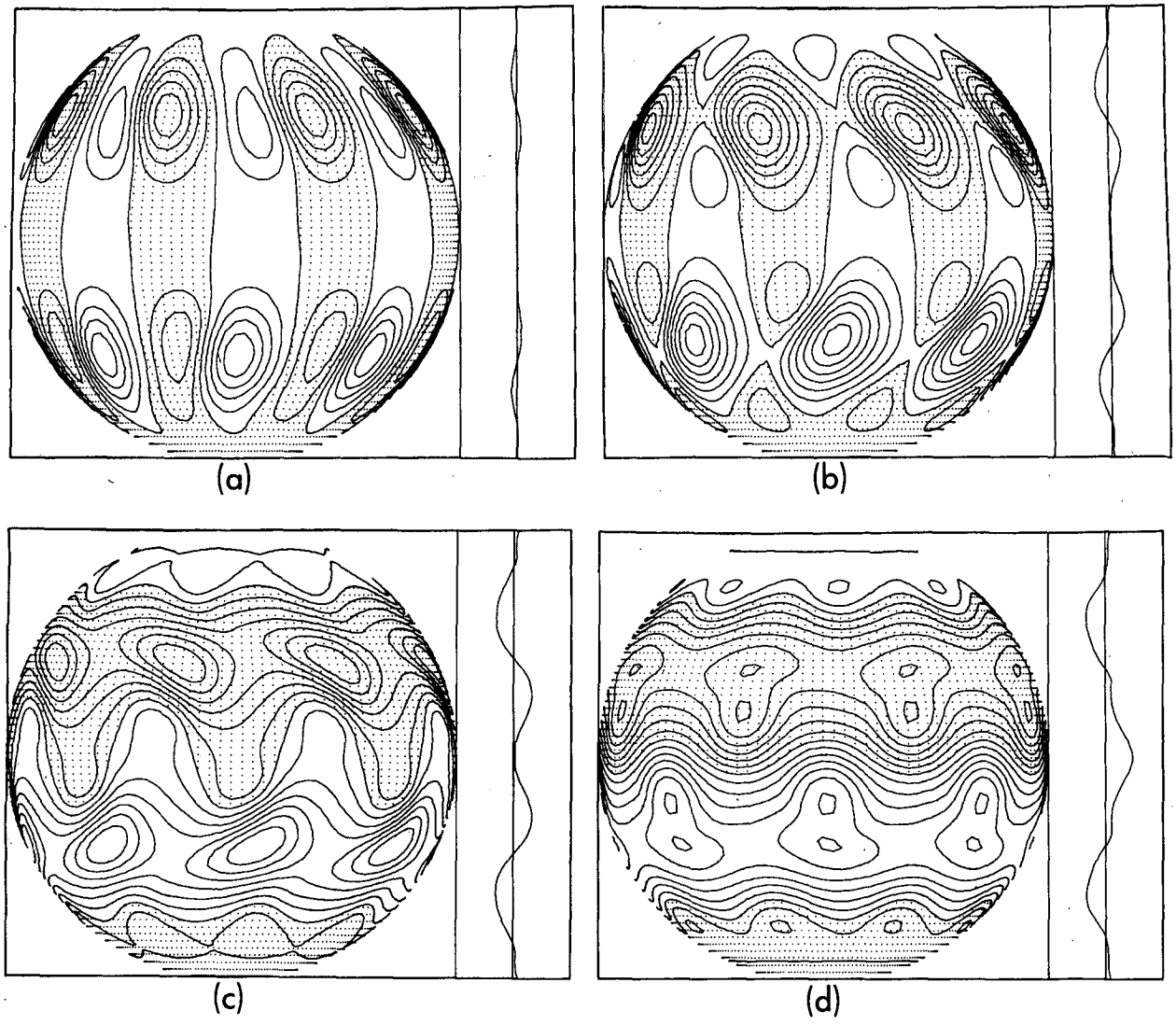

FIG. 6. E1 subcase, $\Omega=0$, streamfunction evolution. Notation as in Fig. 3. $\Delta\psi=10$ km^2 s^{-1}, $u^*=100$ m s^{-1}. Shown at day (a) 5.5, (b) 6.2, (c) 6.9, (d) 10.3.

simplicity of homogeneous forcing, as either homogeneous or inhomogeneous forcing gives the same fundamental easterly-westerly zonal flow. Although calculations were made with a range of parameters, only the results in Table 2 are for those displaying large-scale circulations resembling Jupiter's.

To get some idea of the purely inertial trend of eddy fields in a rotating atmosphere, we first calculate the response of an unforced but initially energetic flow. Theory suggests that zonality is an inertial tendency but its specific manifestation in the absence of forcing is unknown.

a. J1: *Free inertial response*

As shown in Fig. 14a, an initial flow field, $\psi_0=\psi_A$, was constructed with random phase orientation and wavenumbers restricted to $\kappa_0=7$–9 (over the integration domain). The amplitude was such as to give an initial energy level with $|U|\approx 20$ m s^{-1} and a relative vorticity parameter value $\tilde{\beta}=\beta L^2/U\approx 50$, appropriate to the Jovian regime.

Integrating the vorticity equation, with ψ_A as the initial state and with Jovian values of radius and rotation, produces after 115 days the flow shown in Fig. 14b. Nonlinear exchanges have produced larger scale eddies of a predominantly longitudinal orientation. Although weak alternating zonal currents occur at higher latitudes, the flow is not as zonal as in the forced and observed cases, even though the bands have an L_β scale.

Calculation with different initial states—varying the spectral composition and flow amplitude—did not produce flows of any greater resemblance to Jupiter than J1. Although a trend toward zonality appears at

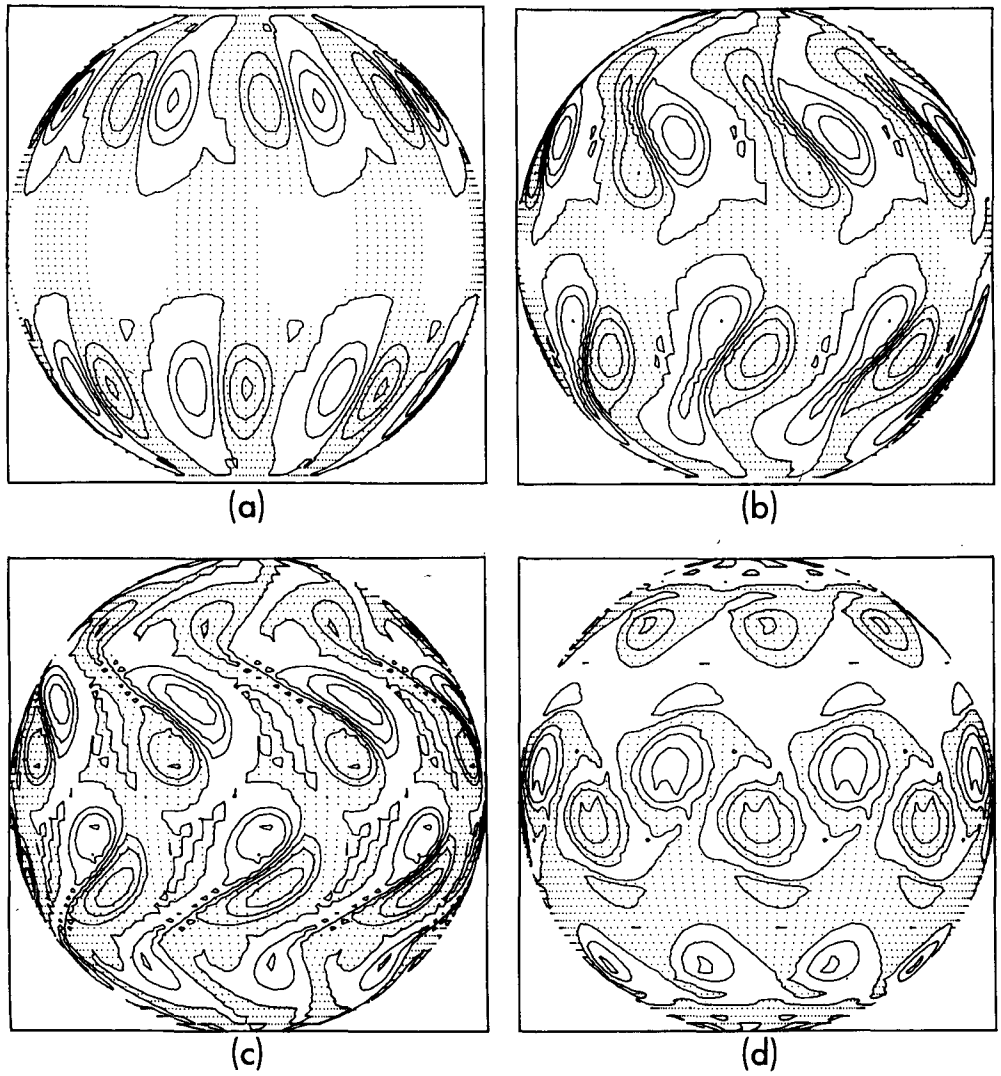

FIG. 7. E1 subcase, $\Omega=0$, vorticity evalution. Notation as in Fig. 3. $\Delta\zeta=4\times10^{-5}$ s^{-1}. Shown at days (a) 4.8, (b) 6.2, (c) 6.9, (d) 10.3.

certain energy levels, the production of zonal jets really requires an active energy source. However, once proper jets have been established they *can* exist freely (see Part 2).

b. J2: *Global forced response*

Case J2 examines the response of an atmosphere of Jupiter's radius and rotation rate to global forcing eddies (Fig. 15) that yield an energy level comparable to that observed. The resulting solution (outlined in Williams, 1975a,b) is the best example of a Jovian circulation obtained with the forced-barotropic model.

As shown in Fig. 16a in the early stages of flow evolution, the motion reflects the forcing. As the energy level increases and energy decascades to larger scales, Rossby-wave propagation sets in at some latitudes (Fig. 16b), and soon becomes global (Fig. 16c). During this transitional stage, from days 23–46, the Rossby waves are steep, indicating that nonlinearity and wave propagation are equally important—as in the Rhines effect.

The transition is rapid, and eddies cease growing as an organized mean zonal flow comes into being (Fig. 16d). Alternating zonal currents, of scale L_β, develop from the waves, with the associated currents and waves moving in the same directions. The coherent phase behavior of Rossby waves provides the necessary organization of the randomly phased eddies to generate mean flows. The ovals at latitude 22° are about half the size of the Great Red Spot; they occur where zonal motion vanishes so would not provide a tracer of atmospheric motion. The flow eventually equilibrates, by lateral dissipation, into a series of highly stable, alternating zonal currents of 50 m s^{-1} magnitude, with little

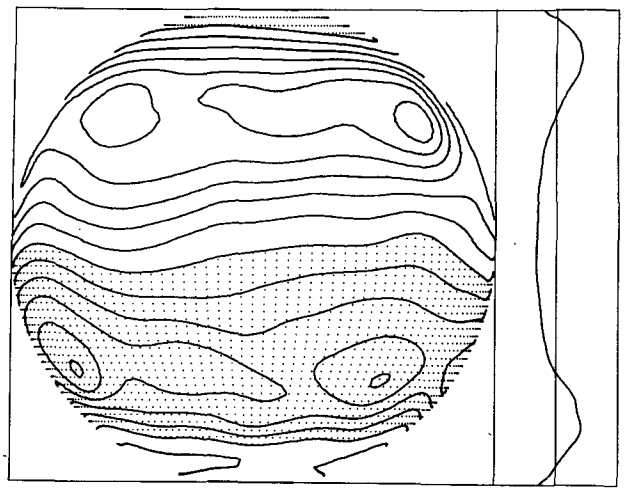

FIG. 8. Case E2, ψ at 31 days, richer forcing mix. $\Delta\psi = 20$ km^2 s^{-1}, $u^* = 100$ m s^{-1}.

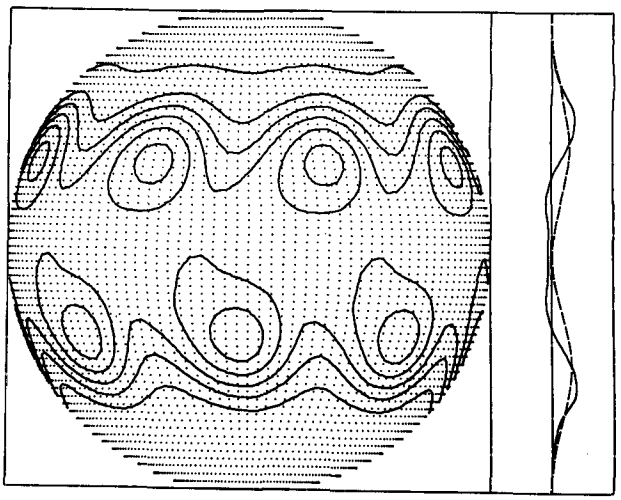

FIG. 10. Case E4, ψ at 43 days, baroclinic supplementary forcing. Additional dotted profile indicates flow form produced by extra forcing component. $\Delta\psi = 20$ km^2 s^{-1}, $u^* = 100$ m s^{-1}.

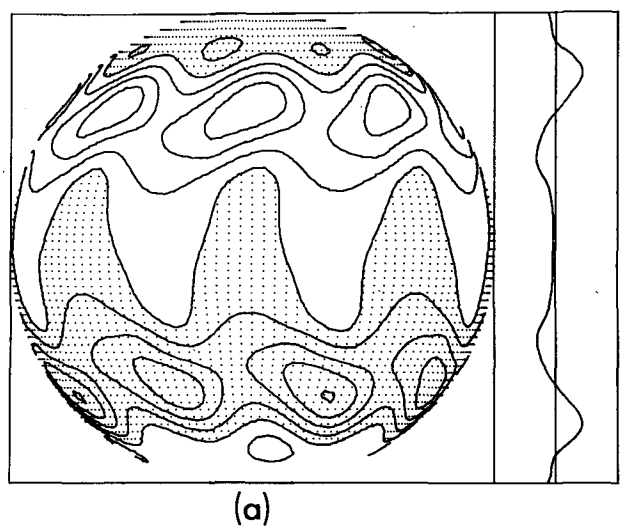

FIG. 9. Case E3, ψ at (a) 23 days and (b) 43.1 days. As in E1 but with surface drag. $\Delta\psi = 20$ km^2 s^{-1}, $u^* = 100$ m s^{-1}.

change occurring from about 120 days to the final 294 days (Figs. 16e and 16f).

The corresponding energy bispectra also reflect the steps in flow evolution. In the initial development (Fig. 17a), the spectrum displays a sharp peak at the forcing scale $k=7$, followed by a spread of energy to a $k=5$ peak as the eddies grow in size (Fig. 17b). The onset of Rossby waves reduces the wavenumber cascade so the spectrum remains peaked at about $k=5$ (Fig. 17c). The later, slower evolution of the spectra mainly illustrates the growth of the zonal flow and the gradual transfer of energy into large scales as the flow gains strength (Figs. 17d and 17e). At the end, the three hemispheric jets dominate the spectrum, with smaller energy scales decaying at the theoretically conjectured k^{-4} state.

c. J3: *Equatorial jet*

An equatorial jet does not occur in the J2 case primarily because the integration domain is hemispheric. We know from the terrestrial solutions E5–E7 that equatorial jets can easily be produced, provided the driving eddies are symmetric about the equator. An alternative possibility for Jupiter is that an enhancement of forcing in the equatorial region can create jets there. This is shown in Case J3 (Fig. 18), in which the forcing amplitude is doubled in the region of $\pm 7°$ latitude. Jets produced by sharp local increases in F tend to drift about the equator; a combination of enhancement and symmetry in the equatorial forcing produces a more rooted flow.

Other calculations failed to produce solutions of any greater similarity to Jupiter's circulation than the above. In particular, varying the forcing wavenumber gave similar results for values of $\kappa = 5$–8 over the 45° domain. At larger κ the flows were less organized, but

this could be due to resolution limitations. Solutions were not sensitive to values of the autocorrelation time τ_F in the 1–10 day range.

d. Discussion

The production of zonal jets and their resemblance (Fig. 16) to the Jovian state is significant considering that only the Jovian geometry, rotation rate, kinetic energy level and driving scale have been imposed. Although the forced-barotropic model appears to produce the main features of the Jovian circulation, the model is only approximate, for as we shall see in the baroclinic model (Part 2) the forcing in a multiple-jet flow is latitudinally inhomogeneous and intermittent. Thus the Jovian circulation should be considered as akin to multiple sets of E1 rather than of E7 flows.

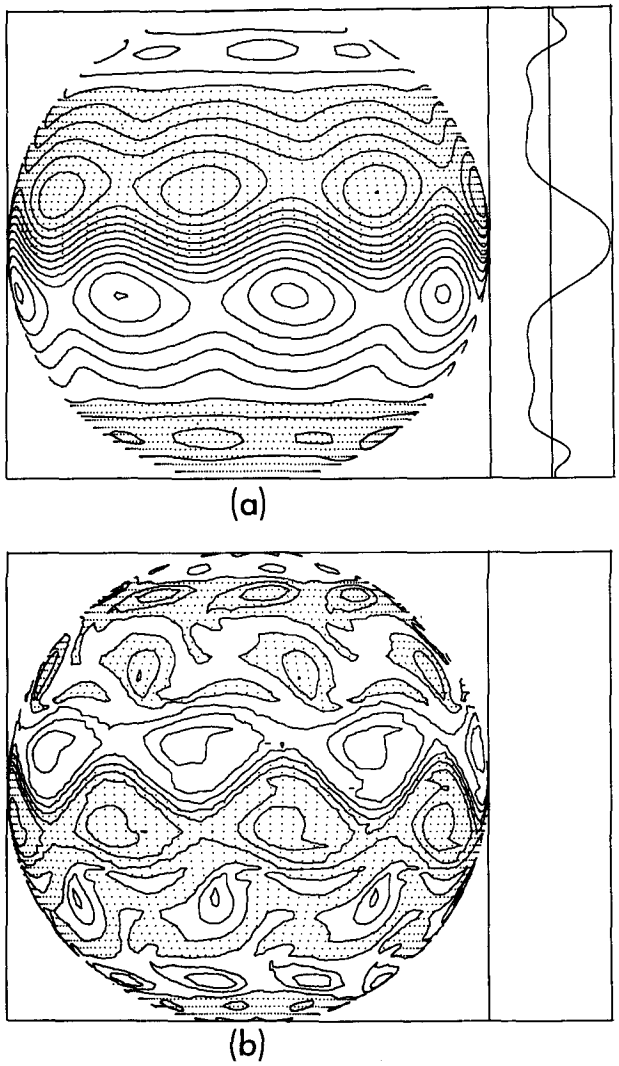

FIG. 11. Case E5. (a) ψ and (b) ζ at 17 days. Hemispherically symmetric forcing (a) $\Delta\psi=20$ km^2 s^{-1}, $u^*=100$ m s^{-1}, (b) $\Delta\zeta=4\times10^{-5}$ s^{-1}.

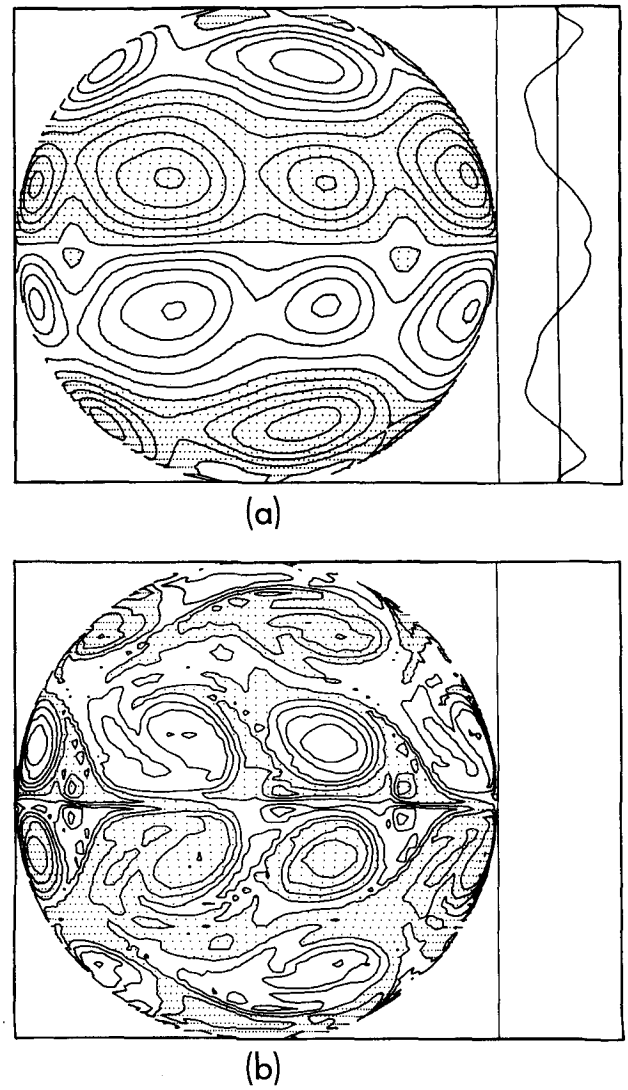

FIG. 12. Case E6. (a) ψ and (b) ζ at 17 days. Hemispherically asymmetric forcing (a) $\Delta\psi=20$ km^2 s^{-1}, $u^*=100$ m s^{-1}, (b) $\Delta\zeta=4\times10^{-5}$ s^{-1}.

The absence of surface drag in the Jovian cases leads to greater zonality in the jets whereas in the terrestrial solutions E3, E4 the drag blocks energy in wavenumbers 1–4 and causes the jets to be less zonal.

e. Cloud formation

Perhaps the most remarkable aspect of the Jovian circulation lies in the visibility of the motions—the constituent gases provide excellent tracers. Although the barotropic model says nothing directly about vertical motion, a barotropic mechanism exists that could produce clouds: Ekman pumping (Charney and Eliassen, 1949). The association of the main cloud bands with the large-scale jet stream flows supports such a

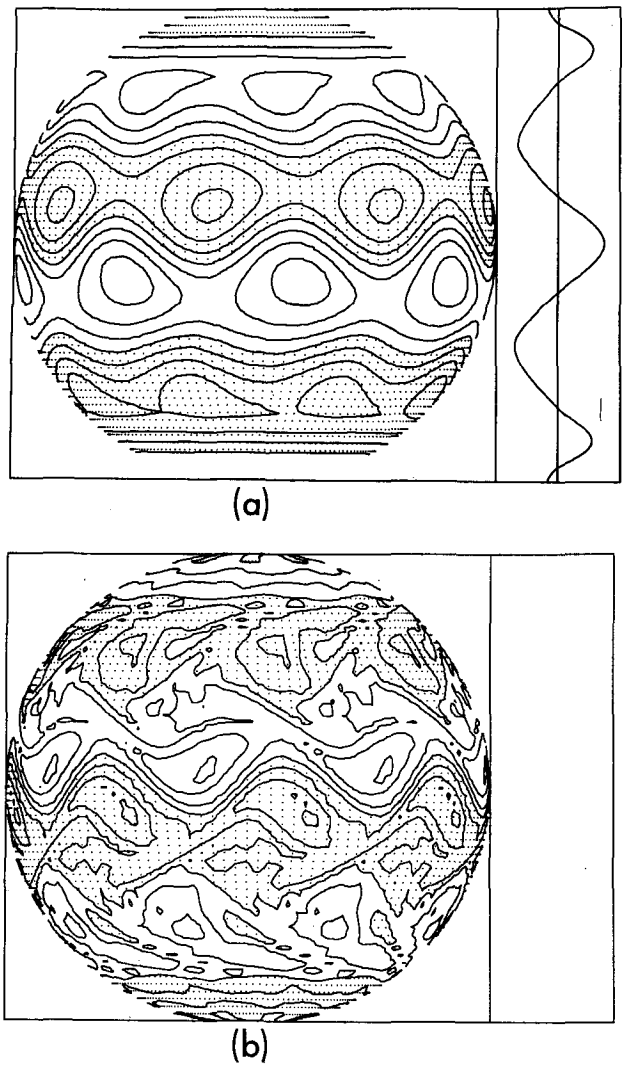

FIG. 13. Case E7. (a) ψ and (b) ζ at 17 days. Transequatorial forcing. (a) $\Delta\psi = 20$ km^2 s^{-1}, $u^* = 100$ m s^{-1}, (b) $\Delta\zeta = 4\times10^{-5}$ s^{-1}.

possibility, but ignorance about the lower interface undermines the suggestion.

In the Ekman process the vertical motion w and large-scale vorticity are related at a lower boundary by

$$w = \frac{h}{f\tau_D}\zeta, \tag{17}$$

where h is the depth of the atmosphere.[9] Thus, the alternating jet streams could frictionally induce a system of alternating cells at some "surface" level, with the Jovian water clouds, if they exist, providing the necessary interface. Ekman layers cannot form at the equator, allowing a possible separate cloud line to form there due to the singularity; such cloud lines are observed. [For the earth, Eq. (17) correctly yields a three-cell system as observed, with the Hadley cell being induced in response to externally driven tropical easterlies—in a moist atmosphere, however, the reverse occurs.)

The relation between w and ζ in (17) correctly implies the existence of differentially rotating bands. From the observed differential rotation, it further suggests that motion is downward in zones, upward in belts. On the other hand, implicit *interpretation* of spectroscopic data suggests that motion is upward in zones, downward in belts. Agreement occurs if Ekman layers form on an upper surface, but it is more likely that the data analysis is incorrect or that other processes prevail.

9. Concluding summary

Solutions that display certain morphological and dynamical similarity (where known) with the observed terrestrial and Jovian circulations have been produced by a simple stochastically forced barotropic vorticity-transfer model. The generation of zonal currents by eddy action, rather than vice-versa, contrasts with the dynamics described by instability theory. The results indicate that, for both atmospheres, barotropic (mechanical) processes control large-scale features, baroclinic (thermodynamical) processes the energy supply and more subtle behavior.

Application of the model to the Earth produced flows with a westerly jet in the forced zone and a uniform easterly wind elsewhere. Although this angular momentum partitioning can be explained in terms of two-dimensional cascades and differential Rossby wave propagation, the relationship with the Rhines effect is complicated by the inhomogeneity of the responsible eddy field. However, by maximum simplification of the forcing such processes can be examined in greater detail—even though they are still nonlinear—than when a more complete simulation is made.

For Jupiter, the solutions support the hypothesis that the zonality and scale of the bands, the oval shaped disturbances and the waves are all essentially characteristics of the quasi-barotropic vorticity exchanges occurring in the two-dimensional turbulence of a rapidly rotating planet. The equatorial jet is considered to be of the same form as the other jets and not a separate phenomenon. This turbulence model for the Jovian circulation is made plausible by the fact that the main features depend only on inertial processes—not on parameterizations—and that the model also applies to the Earth. However, barotropic or quasi-barotropic models cannot explain the Great Red Spot; the reason for this becomes apparent in Part 2 where the gyre is shown to be the warm core of a neutral baroclinic wave.

Concerning the Earth-Jupiter connection, the multiple Jovian jets can be thought of (roughly) as

[9] Boundary layers that form at non-solid surfaces (Hide, 1964) may also be relevant.

TABLE 2. Jovian barotropic calculations. Parameter values for Jovian calculations together with $a=0.7\times10^5$ km, $\Omega=0.176\times10^{-3}$ s^{-1}. D2 and BC3 drag and boundary conditions systems. Resolutions is 128 × 128 except for J3, where 256 points are used over θ.

Case	$\lvert F\rvert$ (s^{-2})	(κ_x,κ_y)	ψ_0	κ_0	ν (km^2 s^{-1})	R_T	θ_-, θ_+	Φ	Δt (s)	Final $\langle u\rangle$ (m s^{-1})
J1	0	—	ψ_A	7–9	0.2	500	−60°, 60°	90°	2500	12
J2	8×10^{-11}	5,5	—	—	0.5	350	0, 80°	45°	2000	32
J3	8×10^{-11}*	5,15	—	—	0.5	200	−80°, 80°	45°	2000	65

* Forcing doubled over ±7° latitude about equator, transition by erf function.

repetitions of the basic jet stream and trade winds of the Earth's atmosphere. This contention is supported by calculations with the baroclinic model showing that multiple jets occur in the terrestrial regime when the planetary rotation rate is increased (see Part 3).

Surface drag is a key item in understanding differences between the two planetary regimes. The strong drag on the Earth's circulation prevents a completely zonal end state from being achieved, whereas its absence or weakness on Jupiter allows energy to cascade more fully into the zonal flow. Yet, the presence of some drag in the Jovian atmosphere may be indicated by the large-scale cloud formation if Ekman pumping is the responsible mechanism.

The production of zonal states by processes other than the axisymmetric instability mechanisms, clears the way for consideration of the non-axisymmetric energy releasing processes.

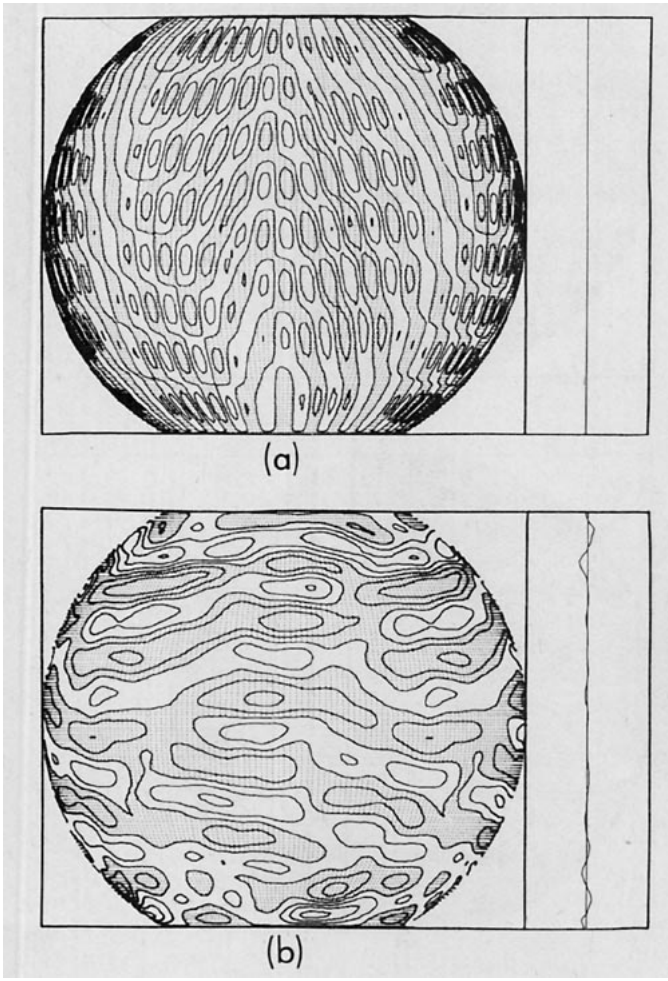

FIG. 14. Case J1. ψ at (a) 0 days and (b) 115 days. Computational sector is repeated for global display. $\Delta\psi=40$ km^2 s^{-1}, $u^*=100$ m s^{-1}.

APPENDIX

Numerical Procedure for Barotropic Model

1) The independent variables x, y correspond to points projected onto a cylinder at the equator. The discretization $x=(i-1)\Delta x$, $y=(j-1)\Delta y$, $i=1, 2, \ldots, M$, $j=1, 2, \ldots, L$, produces equi-spaced grid points in $y(=a\sin\theta)$ that correspond to more widely spaced locations in θ as the poles are approached. This desirable feature results, for example, in our only having to halve the time step when the integration domain is increased from 60° to 85°.

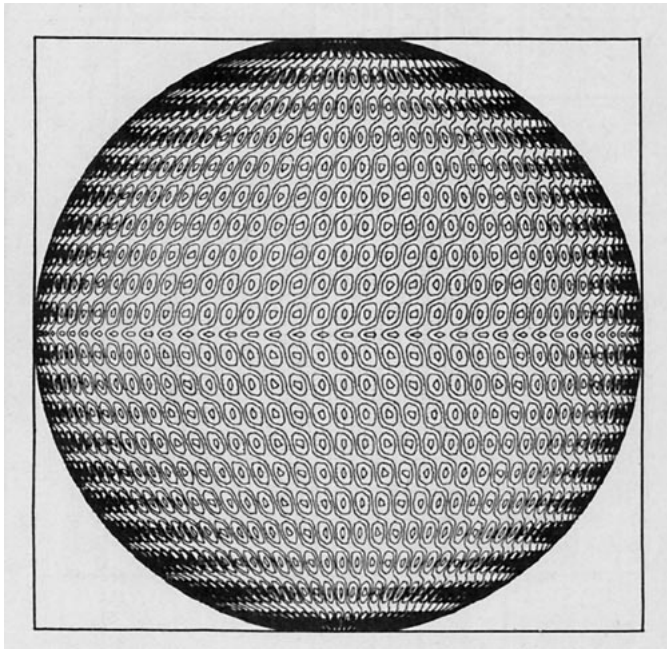

FIG. 15. Case J2. Forcing field F at 73.6 days. $\Delta F=5\times10^{-11}$ s^{-2}.

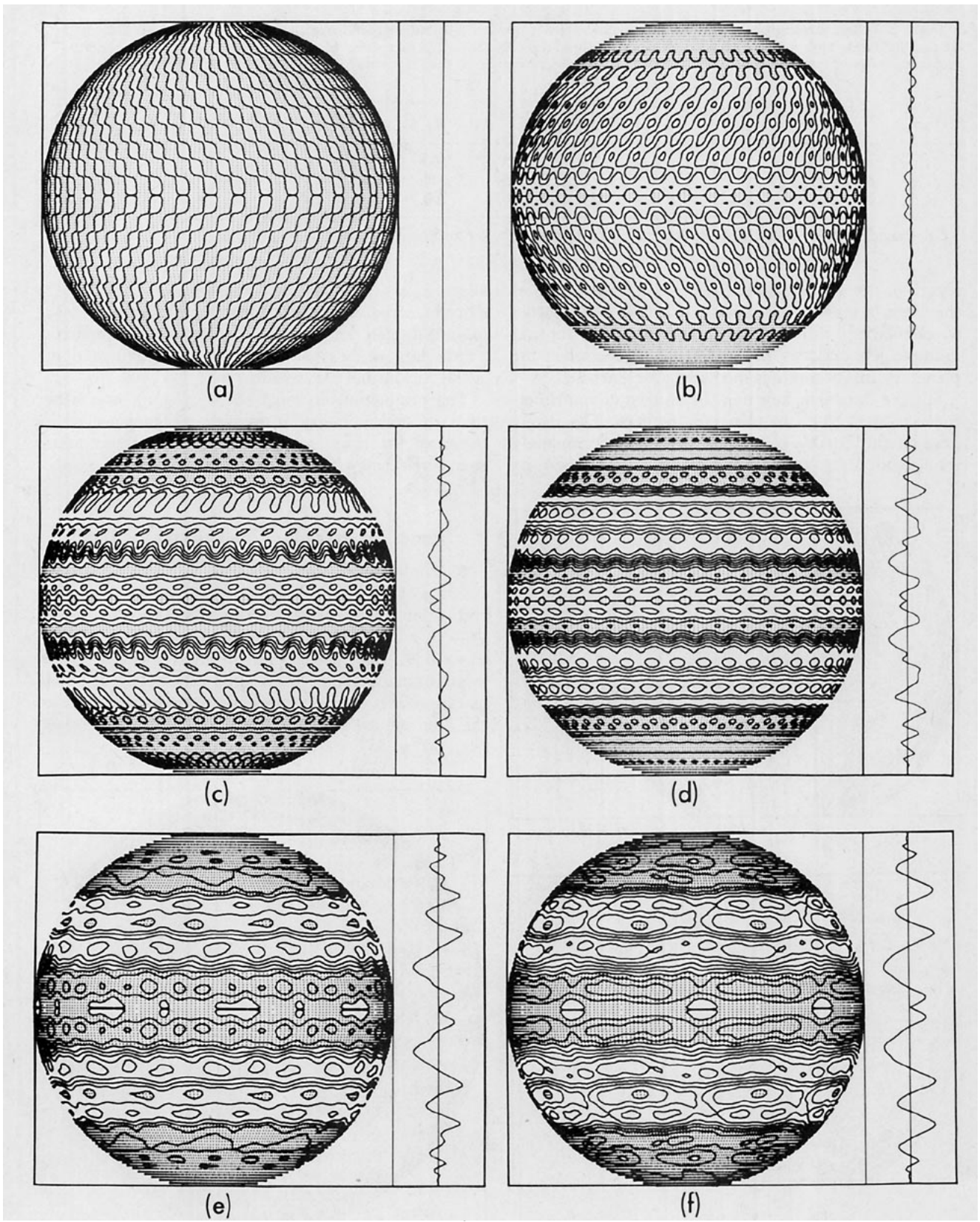

FIG. 16. Case J2. Streamfunction at days (a) 4.6, (b) 23.0, (c) 46.0, (d) 73.3, (e) 161, (f) 294.4. $u^* = 100$ m s^{-1}, (a)–(d) $\Delta\psi = 40$ km^2 s^{-1}, (e)–(f) $\Delta\psi = 80$ km^2 s^{-1}. Computational sector is repeated for global display. A cine version of this solution is available.

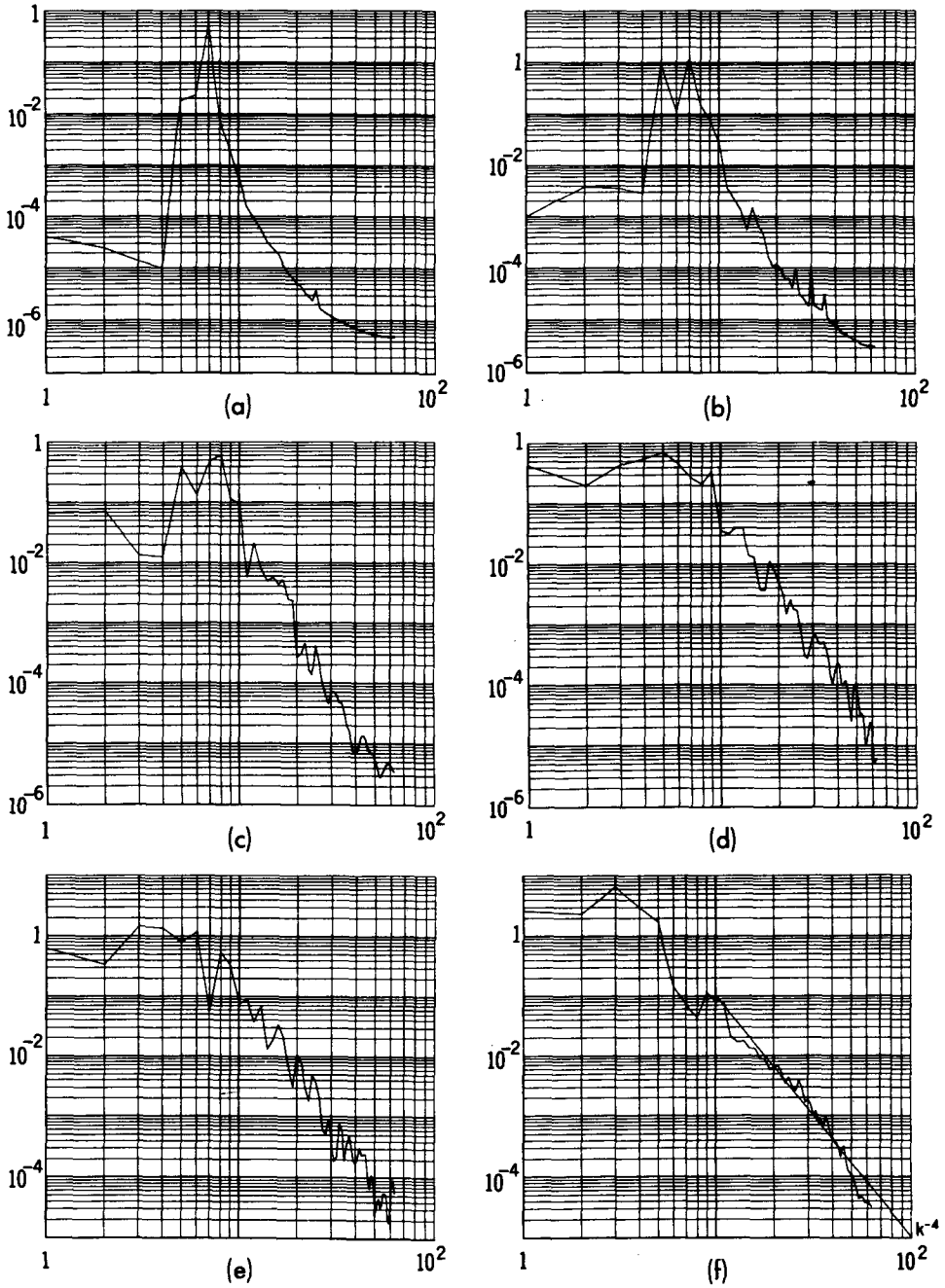

FIG. 17. Case J2. Kinetic energy bispectrum at days (a) 4.6, (b) 13, (c) 23, (d) 46, (e) 74, (f) 294. Abscissa is wavenumber.

2) Eq. (8) becomes, in central difference notation

$$\delta_t\bar{\zeta}^t+J(\psi,\, f+\zeta)=\nu[m^2\delta_{xx}\zeta+\delta_y(m^{-2}\delta_y\zeta)] +F-(\zeta/\tau_D). \quad \text{(A1)}$$

All quantities are at the central time level n, except for the diffusion and drag terms which are evaluated at $n-1$. For the Jacobian term, a form of Arakawa's (1966) expression (45) is used in the interior and of his expressions (73) and (74) for predicting ζ on the latitudinal walls. These formulations preserve integrals of kinetic energy and enstrophy.

3) The streamfunction is obtained by solving the Poisson equation

$$m^2\delta_{xx}\psi+\delta_y(m^{-2}\delta_y\psi)=\zeta. \quad \text{(A2)}$$

4) To solve (A2) exactly, the eigenfunction expansion

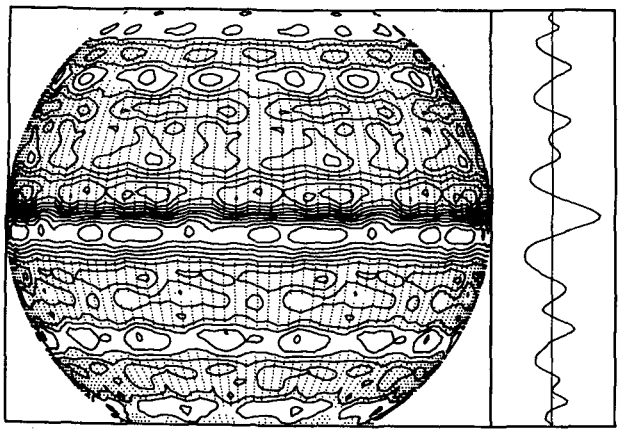

FIG. 18. Case J3. ψ at 147 days. Equatorially enhanced forcing $\Delta\psi=40$ km s^{-1}, $u^*=100$ m s^{-1}. Computational sector is repeated for global display.

is made

$$\psi=\sum_{\alpha=0}^{M-2}\psi^\alpha H_\alpha(i),$$

$$H_\alpha(i)=\Gamma_\alpha\left(\frac{2}{M-1}\right)^{\frac{1}{2}}\cos\left[\frac{2\pi\alpha}{M-1}(i-1)\right],$$

$$\alpha=0,\ 1,\ \ldots,\ (M-1)/2, \quad \text{(A3)}$$

$$H_\alpha(i)=\left(\frac{2}{M-1}\right)^{\frac{1}{2}}\sin\left[\frac{2\pi}{M-1}(i-1)\left(\alpha-\frac{M-1}{2}\right)\right],$$

$$\alpha=\left(\frac{M-1}{2}\right)+1,\ \ldots,\ M-2,$$

where $i=1, 2, \ldots, M$. $\Gamma_\alpha=2^{-\frac{1}{2}}$ for $\alpha=0$ and $(M-1)/2$ (where M is restricted to odd integers of the form $4m+1$), but $\Gamma_\alpha=1$ otherwise. Substitution of (A3) into (A2) yields

$$\delta_y(m^{-2}\delta_y\psi^\alpha)-[m^2/(\Delta x)^2]\lambda^\alpha\psi^\alpha=\zeta^\alpha, \quad \text{(A4)}$$

where

$$\lambda^\alpha=2\left[1-\cos\frac{2\pi\alpha}{M-1}\right], \qquad \alpha=0,\ 1,\ \ldots,\ (M-1)/2,$$

$$\lambda^\alpha=2\left[1-\cos\frac{2\pi}{M-1}\left(\alpha-\frac{M-1}{2}\right)\right],$$

$$\alpha=(M+1)/2,\ \ldots,\ M-2.$$

5) To solve the difference equation (A4) it is written out as

$$-A_j\psi^\alpha_{j+1}+B_j\psi^\alpha_j-C_j\psi^\alpha_{j-1}=D_j, \quad \text{(A5)}$$

where

$$A_j=1,$$

$$B_j=1+\frac{m^2_{j+\frac{1}{2}}}{m^2_{j-\frac{1}{2}}}+\lambda^\alpha\left(\frac{\Delta y}{\Delta x}\right)^2 m_j^2 m^2_{j+\frac{1}{2}},$$

$$C_j=\frac{m^2_{j+\frac{1}{2}}}{m^2_{j-\frac{1}{2}}},$$

$$D_j=-\Delta y^2 m^2_{j+\frac{1}{2}}\zeta^\alpha_j.$$

This equation is solved by using the backward recursion forms E_j, F_j defined as

$$\psi^\alpha_j=\psi^\alpha_{j+1}E_j+F_j,$$
$$E_j=(B_j-C_jE_{j-1})^{-1}, \quad \text{(A6)}$$
$$F_j=E_j(D_j+C_jF_{j-1}).$$

To apply the boundary conditions we write $\psi=\bar{\psi}+\psi'$. The boundary condition systems BC1 and BC2 (Section 6) have $\bar{\psi}=$ constant, $\psi'=0$ on both lateral walls, so the conditions on (A5) are that $\psi^\alpha=0$ when $\alpha\neq 0$ and $\psi^0=\bar{\psi}(M-1)^{\frac{1}{2}}$ for the zeroth mode. The zeroth mode equation degenerates to a simple integral if the velocity condition system BC3 is applied, so that only the condition at one boundary can be imposed, the other is achieved implicitly.

6) Definition of a value of $\bar{\psi}_y$ at the boundaries, for diagnostic purposes or for boundary condition system BC3, is possible through the consistency equations

$$\bar{u}_1=m_1\Delta y\left(\frac{1}{2}\bar{\zeta}_1+\frac{\bar{\psi}_1-\bar{\psi}_2}{m_{1\frac{1}{2}}^2(\Delta y)^2}\right), \quad \text{(A7)}$$

$$\bar{u}_L=-m_L\Delta y\left(\frac{1}{2}\bar{\zeta}_L+\frac{\bar{\psi}_L-\bar{\psi}_{L-1}}{m_{L-\frac{1}{2}}^2(\Delta y)^2}\right), \quad \text{(A8)}$$

derived from the vorticity integral condition equation (11) and the Poisson equation along the lines of Arakawa's (1966) Eqs. (79.1) and (79.2).

7) The trigonometric transforms (A3) and its inverse are evaluated using the so-called fast Fourier transforms. Computations were made using vectorized code on a four-pipe Texas Instruments ASC computer. With the parallel processing of such a computer the relative efficiency of the various Fourier transforms differs from

TABLE A1. Time steps (min^{-1}).

Resolution Y^*X	Barotropic model	Baroclinic model (Parts 2 and 3)
2048^2	1	Not possible
1024^2	5	1
512*128	60	30
256*256	70	35
256*128	100	50
128^2	200	100

that on a serial computer: the efficiency of vectorization increases with larger arrays and this can offset the gain of Fourier techniques that employ reductions in array size. As a result it is preferable to use the standard transform for $M<65$, the Lanczos fourfold way (Williams, 1969) for $M<265$ and the Cooley-Tukey transform for $M>265$, each being optimal in its range.

8) An indication is given in Table A1 of the approximate computational capability (in 1975) of the ASC for the barotropic and two-level baroclinic model of Part 2. Disc transfers are involved.

When predictions of the form $\zeta^{n+1}=\zeta^{n-1}+(\Delta\zeta)^n 2\Delta t$ are required the accuracy in calculating the tendency declines as resolution increases. So although high resolution calculations ideal for turbulence exploration are now possible, the accuracy of the computer is insufficient for calculating the very small tendencies involved with the highest resolutions. Procedures for modifying machine truncation characteristics (Kurihara and Tuleya, 1974) assist in marginal cases.

9) When it becomes necessary to add a random perturbation to induce longitudinal development in a zonal flow, this is accomplished by adding a small random vorticity to the latest value of ζ'. This avoids disruption of the streamfunction and integral constraints.

10) The accuracy of the numerical method and program was tested, in what is now standard procedure, by following the known propagation of the analytic Rossby-Haurwitz wave given by Phillips (1959).

REFERENCES

Arakawa, A., 1961: The variation of general circulation in the barotropic atmosphere. *J. Meteor. Soc. Japan*, **39**, 49–58.

——, 1966: Computational design for long term numerical integration of the equations of fluid motion. *J. Comput. Phys.*, **1**, 119–143.

Arnold, V. I., 1965: Conditions for nonlinear stability of stationary plane curvilinear flows of an ideal fluid. *Dokl. Acad. Nauk. SSSR*, **162**, 773–777.

Batchelor, G. K., 1967: *An Introduction to Fluid Dynamics*. Cambridge University Press, 615 pp.

——, 1969: Computation of the energy spectrum in homogeneous, two-dimensional turbulence. *Phys. Fluids*, **2** (Suppl.), 233–239.

Benjamin, T. B., 1974: Lectures on nonlinear wave motion. *Nonlinear Wave Motion*, A. C. Newell, Ed., *Lectures in Applied Mathematics*, Vol. 15, Amer. Math. Soc., 3–47.

Benney, D. J., 1966: Long nonlinear waves in fluid flows. *J. Math. Phys.*, **45**, 52–63.

——, 1971: Nonlinear waves. *Mathematical Problems in the Geophysical Sciences*, Vol. 1, W. H. Reid, Ed., Amer. Math. Soc., 103–120.

Bretherton, F. P., 1966: Critical layer instability in baroclinic flows. *Quart. J. Roy. Meteor. Soc.*, **92**, 325–334.

——, and D. B. Haidvogel, 1967: Two-dimensional turbulence above topography. *J. Fluid Mech.*, **78**, 129–154.

Chandrasekhar, S., 1943: Stochastic problems in physics and astronomy. *Rev. Mod. Phys.*, **15**, 1–89.

Chapman, C. R., 1969: Jupiter's zonal winds: Variation with latitude. *J. Atmos. Sci.*, **26**, 986–990.

Charney, J. G., 1947: The dynamics of long waves in a baroclinic westerly current. *J. Meteor.*, **4**, 135–163.

——, 1949: On a physical basis for numerical prediction of large-scale motions in the atmosphere. *J. Meteor.*, **6**, 371–385.

——, 1959: On the general circulation of the atmosphere. *The Atmosphere and Sea in Motion*. B. Bolin, Ed., Rockefeller Inst. Press, 178–193.

——, 1963: A note on large scale motions in the tropics. *J. Atmos. Sci.*, **20**, 607–609.

——, 1971: Geostrophic turbulence. *J. Atmos. Sci.*, **28**, 1087–1095.

——, and A. Eliassen, 1949: A numerical method for predicting the perturbations of the middle latitude westerlies. *Tellus*, **1**, 38–54.

Clarke, R. A., 1971: Solitary and Cnoidal planetary waves. *Geophys. Fluid Dyn.*, **2**, 343–354.

Craig, R. A., 1945: A solution of the nonlinear vorticity equation for atmospheric motion. *J. Meteor.* **2**, 175–178.

Dickinson, R. E., 1969: Theory of planetary wave-zonal flow interaction. *J. Atmos. Sci.*, **26**, 73–81.

Eady, E. T., 1949: Long waves and cyclone waves. *Tellus*, **1**, 33–52.

——, 1950: The cause of the general circulation of the atmosphere. *Centenary Proc. Roy. Meteor. Soc.*, 156–172.

Edwards, S. F., 1964: The statistical dynamics of homogeneous turbulence. *J. Fluid Mech.*, **18**, 239–273.

Epstein, E. S., 1969: Stochastic dynamic prediction. *Tellus*, **21**, 739–759.

Ertel, H., 1943: Über stationäre oszillatorische Luftströmungen auf der rotierenden Erde. *Meteor. Z.*, **60**, 332–334.

Fjortoft, R., 1950: Application of integral theorems in deriving criteria of stability for laminar flows and for the baroclinic circular vortex. *Geof. Publ.*, **17**, 1–52.

——, 1953: On the changes in the spectral distribution of kinetic energy for two-dimensional, non-divergent flow. *Tellus*, **5**, 225–230.

Frisch, U., *et al.*, 1974: A Markovian random coupling model for turbulence. *J. Fluid Mech.*, **65**, 145–152.

Gierasch, P. J., 1973: Jupiter's cloud bands. *Icarus*, **19**, 482–494.

Gill, A. E., 1974: The stability of planetary waves on an infinite beta-plane. *Geophys. Fluid Dyn.*, **6**, 29–47.

Godske, C. L., *et al.*, 1957: *Dynamic Meteorology and Weather Forecasting*. Amer. Meteor. Soc., 800 pp.

Golitsyn, G. S., 1970: A similarity approach to the general circulation of planetary atmospheres. *Icarus*, **13**, 1–24.

Green, J. S. A., 1970: Transfer properties of the large-scale eddies and the general circulation of the atmosphere. *Quart. J. Roy. Meteor. Soc.*, **96**, 157–185.

Haltinger, G. J., and R. T. Song, 1962: Dynamic instability in barotropic flow. *Tellus*, **14**, 383–393.

Haurwitz, B., 1949: The instability of wind discontinuities and shear zones in planetary atmospheres. *J. Meteor.*, **6**, 200–206.

Herring, J. R., *et al.*, 1974: Decay of two-dimensional homogeneous turbulence. *J. Fluid Mech.*, **66**, 417–444.

Hess, S. L., 1952: The general atmospheric circulation of Jupiter. Contribution to The Study of Planetary Atmospheres, E. C. Slipher, Ed., Lowell Observatory Rep., Contract AF19 (122)–162, 47–54.

——, and H. A. Panofsky, 1951: The atmospheres of the other planets. *Compendium of Meteorology*, T. Malone, Ed., Amer. Meteor. Soc., 391–398.

Hide, R., 1964: The viscous boundary layer at the free surface of a rotating baroclinic fluid. *Tellus*, **16**, 523–529.

——, 1969: Dynamics of the atmospheres of the major planets etc., *J. Atmos. Sci.*, **26**, 841–853.

Hoskins, B. J., 1974: The role of potential vorticity in symmetric stability and instability. *Quart. J. Roy. Meteor. Soc.*, **100**, 480–482.

Ingersoll, A. P., 1973: Jupiter's Great Red Spot: A free atmospheric vortex. *Science*, **183**, 1346–1348.

——, and J. N. Cuzzi, 1969: Dynamics of Jupiter's cloud bands. *J. Atmos. Sci.*, **26**, 981–985.

Kraichnan, R. H., 1958: A theory of turbulence dynamics. *Proc.*

Second Symp. Naval Hydrodynamics. R. Cooper, Ed., ONR-ACR-38, U.S. Govt. Printing Office, Washington, D.C., 29–43.

——, 1961: Dynamics of nonlinear stochastic systems. *J. Math. Phys.*, **2**, 124–148.

——, 1971: Inertial range transfer in two- and three-dimensional turbulence. *J. Fluid Mech.*, **47**, 525–535.

Kuo, H-L., 1950: The motion of atmospheric vortices and the general circulation. *J. Meteor.*, **7**, 247–258.

——, 1951: Vorticity transfer as related to the development of the general circulation. *J. Meteor.*, **8**, 307–315.

——, 1953: On the production of mean zonal currents in the atmosphere by large disturbances. *Tellus*, **5**, 344–362.

——, 1959: Finite amplitude three-dimensional harmonic waves on the spherical earth. *J. Meteor.*, **16**, 524–534.

Kurihara, Y., and R. E. Tuleya, 1974: Comments on the importance of precision for short range forecasting and climate simulation. *J. Appl. Meteor.*, **13**, 601–602.

Lagrange, J-l., 1781: Memoire sur la theorie du mouvement des fluides. *Nouv. Mem Acad Berlin* (Oeuvres iv), 648–695.

Leith, C. E., 1971: Atmospheric predictability and two-dimensional turbulence. *J. Atmos. Sci.*, **28**, 145–161.

Lilly, D. K., 1969: Numerical simulation of two-dimensional turbulence. *Phys. Fluid*, **11** (Suppl.), 240–249.

——, 1972: Numerical simulation study of two-dimensional turbulence. *Geophys. Fluid Dyn.*, **3**, 289–319.

Loesch, A. Z., 1977: On generation of zonal flows by interacting Rossby waves. *Tellus*, **29**, 306–316.

Long, R. R., 1961: A turbulent equatorial jet. *J. Fluid Mech.*, **11**, 465–477.

——, 1964: Solitary waves in the westerlies. *J. Atmos. Sci.*, **21**, 197–200.

Longuet-Higgins, M. S., 1965: Some dynamical aspects of ocean currents. *Quart. J. Roy. Meteor. Soc.*, **91**, 425–451.

Lorenz, E. N., 1953: The interaction between a mean flow and random disturbances. *Tellus*, **5**, 238–250.

——, 1955: Available potential energy and the maintenance of the general circulation. *Tellus*, **1**, 157–167.

——, 1962: Simplified dynamic equations applied to the rotating basin experiment. *J. Atmos. Sci.*, **19**, 39–51.

——, 1967: *The Nature and Theory of the General Circulation of the Atmosphere*. WMO, 161 pp.

——, 1969: The nature of the global circulation of the atmosphere: a present view. *The Global Circulation of the Atmosphere*, G. A. Corby, Ed., Roy. Meteor. Soc., pp. 2–23.

——, 1972: Barotropic instability of Rossby wave motion. *J. Atmos. Sci.*, **26**, 41–64.

Mak, M-K., 1969: Laterally driven stochastic motions in the tropics. *J. Atmos. Sci.*, **26**, 41–64.

Maxworthy, T., and L. G. Redekopp, 1976a: New theory of the Great Red Spot from solitary waves in the Jovian atmosphere. *Nature*, **260**, 509–511.

——, and L. G. Redekopp, 1976b: A solitary wave theory of the Great Red Spot and other observed features in the Jovian atmosphere. *Icarus*, **29**, 261–271.

McIntyre, M. E., 1970a: Diffusive destabilization of the baroclinic circular vortex. *Geophys. Fluid Dyn.*, **1**, 19–57.

——, 1970b: On the non-separable baroclinic parallel flow instability problem. *J. Fluid Mech.*, **40**, 273–306.

Neamtan, S. M., 1946: The motion of harmonic waves in the atmosphere. *J. Meteor.*, **3**, 53–56.

Newell, A. C., 1969: Rossby wave packet interactions. *J. Fluid Mech.*, **35**, 255–271.

Onsager, L., 1949: Statistical hydrodynamics. *Nuovo Cimento*, **6** (Suppl.), 279–287.

Pedlosky, J., 1964: The stability of currents in the atmosphere and the ocean; Parts I and II. *J. Meteor.*, **21**, 201–219, 342–353.

Phillips, N. A., 1956: The general circulation of the atmosphere: A numerical experiment. *Quart. J. Roy. Meteor. Soc.*, **82**, 123–164.

——, 1959: Numerical integration of the primitive equations on the hemisphere. *Mon. Wea. Rev.*, **87**, 333–345.

Rhines, P. B., 1973: Observations of the energy-containing oceanic eddies and theoretical models of waves and turbulence. *Bound.-Layer Meteor.*, **4**, 345–360.

——, 1975: Waves and turbulence on a beta plane. *J. Fluid Mech.*, **69**, 417–443.

——, 1977: The dynamics of unsteady currents. *The Sea: Ideas and Observations on Progress in the Study of the Seas*, Vol. 7, E. D. Goldberg, Ed., Wiley, 189–318.

Rossby, C. G., 1945: The scientific basis of modern meteorology. *Handbook of Meteorology*, F. A. Berry and E. Bollay, Eds., McGraw-Hill, 501–529.

——, 1947: On the distribution of angular velocity in gaseous envelopes under the influence of large scale horizontal mixing processes. *Bull. Amer. Meteor. Soc.*, **28**, 53–68.

——, 1949: On the nature of the general circulation of the lower atmosphere. *The Atmosphere of the Earth and Planets*, G. P. Kuiper, Ed., The University of Chicago Press, 16–48.

Silberman, I., 1954: Planetary waves in the atmosphere. *J. Meteor.*, **2**, 27–34.

Smagorinsky, J., 1963: General circulation experiments with the primitive equations. I. The basic experiment. *Mon. Wea. Rev.*, **91**, 99–164.

——, 1969: Numerical simulation of the global atmosphere. *The Global Circulation of the Atmosphere*, G. H. Corby, Ed., Roy. Meteor. Soc., 24–41.

Stokes, G. G., 1842: On the steady motion of incompressible fluids. *Cambridge Phil. Soc.*, **7**, 439–455.

Stone, P., 1967: An application of baroclinic stability theory to dynamics of the Jovian atmosphere. *J. Atmos. Sci.*, **24**, 642–652.

——, 1971: The symmetric baroclinic instability of an equatorial current. *Geophys. Fluid Dyn.*, **2**, 147–164.

Taylor, G. I., 1915: Eddy motion in the atmosphere. *Phil. Trans. Roy. Soc. London*, **A240**, 1–26.

Thompson, P. D., 1948: The propagation of permanent-type waves in horizontal flow. *J. Meteor.*, **5**, 166–168.

Walton, I. C., 1975: The viscous nonlinear symmetric baroclinic instability of a zonal shear flow. *J. Fluid Mech.*, **68**, 757–768.

Williams, G. P., 1968: Thermal convection in a rotating fluid annulus: Part 3. *J. Atmos. Sci.*, **25**, 1034–1045.

——, 1969: Numerical integration of the three-dimensional Navier-Stokes equations for incompressible flow. *J. Fluid Mech.*, **37**, 727–750.

——, 1970: Axisymmetric annulus convection at unit Prandtl number. *Geophys. Fluid Dyn.*, **1**, 357–369.

——, 1971: Baroclinic annulus waves. *J. Fluid Mech.*, **49**, 417–449.

——, 1975a: Some ocean-Jupiter connections. *Mode News*, No. 78.

——, 1975b: Jupiter's atmospheric circulation. *Nature*, **257**, 778.

——, and J. B. Robinson, 1973: Dynamics of a convectively unstable atmosphere: Jupiter? *J. Atmos. Sci.*, **30**, 684–717.

Yaglom, A. M., 1962: *Stationary Random Functions*. Dover, 235 pp.